Fall 2022

Species Distribution and Abundance of Bering Sea Tunicates with Implications for Coastal Food Security

Meghan Bugaj
Western Washington University, megbugaj@gmail.com

Species Distribution and Abundance of Bering Sea Tunicates with Implications for Coastal Food Security

By

Meghan Bugaj

Accepted in Partial Completion

of the Requirements for the Degree

Master of Science

ADVISORY COMMITTEE

Dr. Kathryn Sobocinski, Chair

Dr. Leo Bodensteiner

Dr. Lyle Britt

GRADUATE SCHOOL

David L. Patrick, Dean

Master’s Thesis

In presenting this thesis in partial fulfillment of the requirements for a Master’s degree at Western Washington University, I grant to Western Washington University the non-exclusive royalty-free right to archive, reproduce, distribute, and display the thesis in any and all forms, including electronic format, via any digital library mechanisms maintained by WWU.

I represent and warrant this is my original work and does not infringe or violate any rights of others. I warrant that I have obtained written permissions from the owner of any third party copyrighted material included in these files.

I acknowledge that I retain ownership rights to the copyright of this work, including but not limited to the right to use all or part of this work in future works, such as articles or books.

Library users are granted permission for individual, research, and non-commercial reproduction of this work for educational purposes only. Any further digital posting of this document requires specific permission from the author.

Any copying or publication of this thesis for commercial purposes, or for financial gain, is not allowed without my written permission.

Meghan Bugaj

11/28/22

Species Distribution and Abundance of Bering Sea Tunicates with Implications for Coastal Food Security

A Thesis

Presented to

The Faculty of

Western Washington University

In Partial Fulfillment

Of the Requirements for the Degree

Master of Science

By

Meghan Bugaj

November 2022

ABSTRACT

The use of sessile macroinvertebrates as leading indicators of change in marine ecosystems makes them potentially valuable as a management tool for predicting habitat suitability for more mobile, commercially important fishes. In addition to potential use as an ecosystem indicator in fisheries management, tunicates are used as a food resource by some Alaska Native communities. Variability in abundance and distribution, driven by changing physical conditions in the Bering Sea, could impact food security for these communities. I used fishery-independent NOAA survey data from the Eastern Bering Sea summer surveys from 1987 to 2019 to examine abundance and distribution of several tunicate species complexes (*Halocynthia*, *Styela*, and *Boltenia*) in a spatiotemporal modeling framework. Prior to fitting the models, I determined that frequency of occurrence (FoO) and catch per unit effort (CPUE) varied spatially between warm (2015-2019) and cool (2005-2010) periods for all three species. Summary statistics showed declines in biomass for all three species during a relatively warm period. Based on the literature and these preliminary analyses I hypothesized that distributions and abundances of tunicate species would shift with multiyear changes in benthic conditions, especially temperature. Given warming trends and the relatively shallow water found in the Northern Bering Sea (NBS), I expect a disproportionate negative impact on benthic communities in this region. As tunicate species are a significant proportion of the benthic community in this ecosystem, there may be a large impact on coastal Alaska Native communities' ability to harvest an important food resource. Additionally, relationships between environmental conditions, tunicate abundance, and fish distribution and abundance could lead to improved management.

Acknowledgments

I’d like to thank my advisor, Dr. Kathryn Sobocinski, and my committee members Dr. Leo Bodensteiner and Dr. Lyle Britt. Thanks to the National Oceanic and Atmospheric Association (NOAA), -Alaska Fisheries Science Center’s (AFSC) Resource Assessment and Conservation Engineering (RACE) division for providing the data, and to the Western Washington Graduate School for supporting this research.

Contents

List of Figures and Tables

1.INTRODUCTION

Climate change is the most pressing issue facing our planet, with strong implications for the integrity of existing marine ecosystems. Sustained increases or decreases in temperature from the mean can lead to changes in distributions of individual plant and animal populations through extirpation and colonization while seeking their thermal optima (Morley et al. 2018, Spies et al. 2020, Stevenson and Lauth 2012); in turn, altering community composition (Lin et al. 2018). Climate change is disproportionately affecting the polar regions where temperatures are increasing at higher rates than the mid latitudes (Marshall et al. 2014). Organisms in these regions are often already occurring at the extreme end of their thermal tolerance and have nowhere else to go as temperatures warm further (Free et al. 2019, Pinsky et al. 2019). In addition to the trend in increasing temperatures in the northern latitudes there is also more climate and weather variability in year-to-year conditions, making it more difficult to forecast future conditions. The ability to better assess how economically and culturally important Alaskan fisheries and ecosystems are being impacted by climate change, as well as predict how future conditions will impact them, is of primary concern in fisheries management.

The Bering Sea is a mostly enclosed marginal sea that forms the divide between the United States and Russia. It covers 772,200 square miles and is an important location for studying connectivity between the Pacific and Arctic Oceans (Clement et al. 2005). The Anadyr and Yukon rivers are major sources of fresh water into the Bering Sea (Clark and Mannino 2022). The U.S. Bering Sea boasts a $1 billion fishery (NOAA Fisheries 2022) for many species such as Pacific Cod (*Gadus macrocephalus)*, Pollock

(*Theregra chalcogramma),* Bristol Bay Sockeye Salmon (*Oncorhynchus nerka)*, Pacific Halibut (*Hippoglossus stenolepis)*, Red King Crab (*Paralithodes camtschaticus),* Opilio Crab *(Chionoecetes opilio)* and other groundfish and invertebrates. The Russian−controlled waters support a $600 million fishery (NOAA Fisheries 2022). The Northern Bering Sea (NBS) is closed to commercial bottom trawling (though not entirely closed to commercial fishing, longline and pot fisheries are permitted in the region) while the Eastern Bering Sea (EBS) is heavily trawled.

Climate change in the Bering Sea is affecting environmental conditions that have historically existed in the area. The cold pool is unique to the EBS, describing the area with cold near-bottom waters (less than -2 °C). During cold years the cold pool can persist year-round, while during warm years it breaks down completely (Wyllie-Echeverria and Wooster 1998). Cold Pool Extent (CPE) is an oceanographic index determined by the amount of sea ice in late winter and spring and is used to track climate change in the area (Wyllie-Echeverria and Wooster 1998). Warmer temperatures allow for less formation of sea ice in late winter and spring, and August 2018 saw the lowest CPE on record (Stabeno and Bell 2019). Including CPE in statistical models explains larger amounts of spatial variation in several fish and invertebrate species distributions and abundances than temperature alone, suggesting it is an important structuring variable (Thorson 2019). Fish distributions are impacted by the spatial extent of the cold pool as well as the timing of cold pool formation and dissolution, with sub-arctic species avoiding bottom waters less than 1°C (Thorson 2019). CPE can be used as a direct measure of climate change in the EBS.

In addition to the CPE, the Bering Sea is demonstrating temporal trends in ocean condition researchers refer to as “stanzas” (Stevenson and Lauth 2019). These stanzas mark a shift from high interannual variation in temperature observed at the beginning of the time series (from 1987 to about 2004) to prolonged periods of bottom temperatures that are either higher or lower than the mean temperature for the baseline (the first 17 years). The period from 2005 to 2010 marks a cold stanza, while that from 2015 to 2019 marks a period of warmer than average temperatures, a warm stanza. In addition to an overall warming trend, in the most recent 15 years of data there is a trend towards increased variation in temperature from the mean (Stevenson and Lauth 2019). Understanding distribution change in “stanzas” of relatively cold and warm water could shed light on longer-term thermal preference of organisms. Distribution and abundance patterns at the end of the cold stanza (2010) versus the end of the warm stanza (2019 in this dataset, presumably still getting warmer in the present) may reveal differences in survival under differing stanzas.

Sessile invertebrates form important benthic communities, changing the environments they live in through the creation of biogenic habitat for other invertebrates or juvenile fish (Francis et al. 2014, Nadtochy et al. 2017). Sessile invertebrate assemblages also demonstrate the effects of bottom trawling on an area. Predicted distributions of sponges, cold-water corals, and sea pens in the Nordic seas have been used to accurately predict the distribution of vulnerable marine ecosystems or VMEs (Burgos et al. 2020). VME is a designation used to describe regions that would be particularly damaged by bottom trawling and are therefore deserving of regional and federal protection in fisheries policy.

The ascidians *Halocynthia aurantium* (sea peach) and *Boltenia ovifera* (sea onion) have been used to predict VMEs in the Anadyr region of the Bering Sea in the Russian controlled waters (Nadtochy et al. 2017). Ascidians in general have declined in frequency of occurrence (FoO) in this same region between 1895 and 2005 as determined by benthic grab samples (Grebmeier et al. 2006). The fact that large-scale trawling is not prominent in this region makes other factors, such as climate shifts, more compelling as drivers of biomass change to which the invertebrates might respond. It is unknown how sessile invertebrates might respond to an expanding or contracting cold pool in the Bering Sea, but they may serve as indicators of environmental conditions, especially in the northern seas due to their inability to move to more optimal environments (Burgos et al. 2020, Nadtochy et al. 2017).

Tunicates are colonial or solitary ascidians or “sea squirts”—so called for their incurrent and excurrent siphons. They are exclusively found in marine environments. Solitary ascidians make up around 40% of named ascidian species, and they tend to dominate in colder water (Shenker and Swalla 2011), with colonial species making up most tropical populations. Historically, solitary ascidians have made up a large proportion of the epibenthic fauna in regions of both the EBS and NBS. They are filter feeders with a circumpolar distribution and have primarily been studied in terms of their likely position as a “sister group” to the vertebrates (Lemaire and Piette 2015) or for their pelagic species invasions into waters where they are not endemic (Pettitt-Wade et al. 2020).

Little is known about tunicate life history and ecology in the Bering Sea, but as sessile invertebrates their distribution is driven by dispersal from reproduction.

Tunicates exhibit different reproductive patterns based on latitude. In more temperate latitudes there is usually one spawning event a year, while in the tropics spawning is more continuous (Ferrero et al. 2019). This suggests a possible role of temperature in spawning frequency; tunicate population sizes may be sensitive to changing temperatures. All ascidians are hermaphrodites and bear lecithotrophic larvae, and all solitary ascidians reproduce only sexually, most releasing gametes to the environment for external fertilization and larval development (Ferrero et al. 2019). Therefore, the spatial distribution of solitary tunicates is a result of local oceanography and larvae seeking suitable places to settle. Tunicate larvae settle relatively quickly, spending no more than a few days in the water column (Ferrero et al. 2019).

This study focuses on three species complexes of solitary, sessile, tunicates native to the Bering Sea: *Boltenia ovifera* (the sea onion), *Halocynthia aurantium* (the sea peach) and *Styela rustica* (the sea potato). These species are the most abundant collected in groundfish surveys in the Bering Sea and are all important to Native communities in the Bering Strait region as a subsistence food resource called “Oopa” featured in holiday celebrations (L. Britt, NOAA RACE division, personal communication, September 2020, Lambert et al. 2016). They are added to stews, frozen whole and thinly sliced and consumed with crystalized briny water from inside, or blanched and peeled before consumption. Oopa or Upa (as they are called in Russia) are of particular importance to the Savoonga and Gambell communities on St. Lawrence Island, Diomede on Little Diomede Island, Wales, Shishmaref, and Teller (L.Britt, NOAA RACE division, personal communication, November 2022). Novy Chaplino in Russia hosts an annual “Upafest” where there are competitions for the

largest caught ascidian and cook outs of local sea-squirt dishes. As a sought-after food resource, tunicate availability (via abundance and distribution) has food security implications for the coastal Native communities in the region. With changing temperatures potentially influencing dispersal, understanding tunicate response to changing ocean conditions is a priority for food security and fisheries management.

To understand changes in species distribution and abundance researchers often use species distribution models (SDMs). SDMs have emerged as a popular way to quantify species distributions in marine, terrestrial, and freshwater environments over time and/or in response to ecological covariates; additionally, they are used to make predictions extending beyond the study region (Elith and Leathwick 2009). Within fisheries science, maximum entropy (MaxEnt) SDM models have been used to relate presence-only data of Atlantic Herring, Atlantic Mackerel, and Butterfish to several environmental covariates to accurately hindcast occurrence (Wang et al. 2018). Generalized Linear Models (GLMs) have accurately predicted rockfish distributions on the California coast (Young et al. 2010). Using a 36-year fishery-independent survey in Texas estuaries, researchers found that abundance on both a seasonal and long-term scale could be accurately predicted using boosted regression trees (BRTs; Froeschke & Froeschke 2016). Ecological data are often collected over time and across varying spatial scales, suggesting that both time and space play a role in species distributions, sometimes tied to environmental conditions (Barnett et al. 2021).

SDMs can be fitted using a variety of spatially and temporally explicit data. Tunicates are commonly collected in demersal fish surveys using bottom trawls and are incidental catch in NOAA’s annual groundfish surveys in Alaska. As such, we have

many years of data on their catch per unit effort (CPUE) at specific stations throughout the EBS and NBS. SDMs can be used with fishery-independent data as described above or with fishery-dependent data collected by onboard observers on commercial fishing vessels (Karp et al. 2022). Data collected over broad spatial scales and across long time series are particularly useful as they incorporate changing environmental conditions.

State-space models relate observations of a response variable to unobserved (latent) “states” or “parameters” such as time or geographic location (Durbin and Koopman 2012). Species distribution models (SDMs) are a type of state-space model in that they relate either presence/absence or biomass of a taxon to chosen covariates. State-space SDMs, such as species distribution model template model builder (sdmTMB; Anderson et al. 2022) or vector autoregressive spatiotemporal model (VAST; Thorson 2019), allow investigation of relationships in distribution across space and time. These models have typically been used on fishery-independent survey data because fisheries surveys are typically conducted during consistent seasons with consistent effort making them comparable across time (Elith and Leathwick 2009, Essington et al. 2022, Evans et al. 2021, Ward et al. 2022). Due to the temporal nature of climate change, these types of models are applicable to understanding the effects of climate change on species distributions.

To investigate changing distributions and abundances of tunicates in the Bering Sea, I used spatiotemporal (state-space) statistical models. This work focuses on the abundance (CPUE) based SDMs because a focus on occurrence-based (presence/absence) models could miss the importance of species present in high

numbers at a small number of sites (Winfree et al. 2015). CPUE changes also might serve as timelier indicators of impending population crashes due to environmental conditions, especially in sessile animals, because frequency of occurrence patterns will not change until the population is already extinguished (Clements et al. 2017) at which time the information will be less useful in fisheries management. Fishing behavior can be adjusted if we can recognize areas of the Bering Sea that host organisms more vulnerable to additional trawling pressure in the face of warming temperatures.

I predicted the frequency of occurrence (presence/absence) and catch per unit effort (in kilograms/ ha) for the three tunicate species each year across the EBS and NBS, interpolating between stations for which I have data. Time served as a proxy for temperature to account for the warm and cold stanzas evaluated in this study (Stevenson and Lauth 2019). Because the NBS is untrawled, like the Anadyr region, any changes seen here could be attributable to climate change (Nadtochy et al. 2017). I hypothesized that a) tunicate abundances and distributions will be different between the end of the cold stanza (2010) and the end of the warm stanza (2019). Based on the literature and preliminary analyses I anticipated higher overall abundances at the end of the cold stanza than at present. I expected distributions to become more localized as water in the Bering Sea warms. I also predicted b) that changes, particularly in distribution, would be more pronounced at northern latitudes due to shallower, warmer water, potentially creating food security issues for the people living there who rely on tunicates as a food source both culturally and for subsistence. Tunicate populations may establish further offshore seeking relatively deeper, cooler water corroborating reports of people in the area of decreased abundance nearshore for harvest.

2. MATERIALS AND METHODS

2.1 Study Area

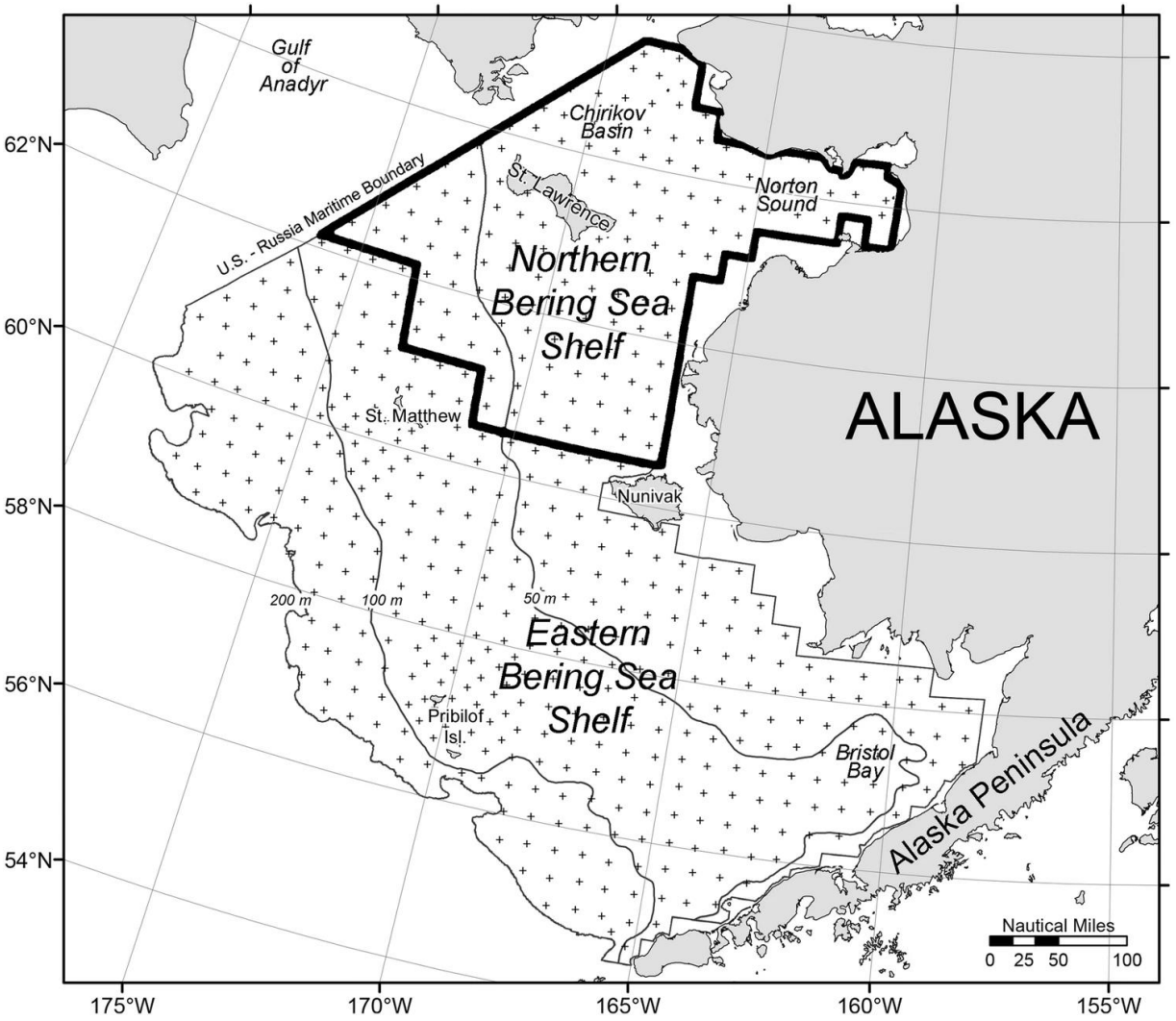

Figure 1: Map of the Bering Sea depicting the Eastern and Northern Bering Sea regions and major geographic features. Crosses indicate individual sampling stations for the NOAA Fisheries Bering Sea groundfish survey- (Stevenson and Lauth 2019).

This study was carried out in the Eastern Bering Sea, bordered by the United States to the east and Russia to the west (Figure 1). The Bering Sea includes Exclusive Economic Zones belonging to both countries, as well as an international zone in the center often referred to as “The Donut Hole”. Figure 1 depicts the U.S.−controlled

portions of the Bering Sea. The area along the continental shelf in the northern and eastern parts of the Sea is typically shallower than 200 m, with the 200-m isobath determining the shelf break. The deepest point is in a southwestern portion of the Bering Sea outside of U.S. controlled waters in Bower's Basin and reaches about 4000 m. The Sea contains several islands, 16 submarine canyons, and four primary regions: the Bering Strait, Bristol Bay, the Gulf of Anadyr, and Norton Sound. For the purpose of this work the EBS is defined as the region from the Alaska Peninsula to 60°N located within U.S. territorial waters and is the focus area of most of the U.S. fisheries survey effort in the Bering Sea. The NBS is defined as the region from 60°N to 65°N within U.S. territorial waters and is bounded by the Bering Strait to the north.

2.2 Data Collection

The location (haul start latitude and start longitude), catch per unit effort (kg/ha), bottom temperature (ºC), and bottom depth (m) data were collected during a fishery–independent bottom trawl survey conducted annually by the National Oceanic and Atmospheric Association (NOAA), Alaska Fisheries Science Center's (AFSC) Resource Assessment and Conservation Engineering (RACE) division from 1987 to 2019. Survey trawl protocols are detailed in Stauffer (2004) and will be briefly outlined here. The basic set-up consists of an Eastern otter trawl with 102-mm stretched mesh body, 89-mm stretched mesh intermediate, 32-mm mesh codend liner, 25.3-m headrope, and 34.1-m footrope (Stauffer 2004). The trawl opening is spread by 1.8-m x 2.7-m steel doors. The net opening width averages about 16 m, and distance towed averages 2.77 km per haul based on tows of approximately 30- minutes. Much work has gone into making survey

data collection as standardized as possible so that it is comparable over time and to other geographic regions.

There are 520 stations sampled each year with a single trawling effort (Figure 1), with most station depths falling between 25 and 75 meters. Not all stations are sampled every year. In only three of the 33 years (2010, 2017, 2019) the survey was extended into the NBS, resulting in fewer samples for this region but allowing several years for comparison. The response variable, abundance of species, has been standardized to Catch Per Unit Effort (CPUE) in kilograms per hectare. These values were calculated by dividing the catch weight by the area swept by the trawl; the area swept is equal to the product of the mean net width and the distance towed. CPUE was chosen as the response variable of interest over counted abundance as tunicates can be difficult to count and often come up in pieces during trawl surveys.

Tunicate species were narrowed down to the three most frequently occurring species complexes after looking at the relative abundance across the time series of all tunicates in the survey data. The *Boltenia* complex is almost exclusively *Boltenia ovifera* (the sea onion) although *B. ecinata* is also present. *Halocynthia* is primarily *Halocynthia aurantium* (the sea peach). *H. igaboja* and *H. hispidus* are also present in very small numbers in some years. *Styela* is assumed to be made up entirely of *Styela rustica* (the sea potato). Invertebrate identification confidence has improved over the time series (Stevenson and Hoff 2009), and sorting species into these broader species complexes alleviates the misidentification of rarer species, especially early in the time series.

2.3 Temperature and Stanzas

To better understand temperature patterns over the time series and to determine whether the stanzas noted in Stevenson and Lauth (2019) were evident in these data, I evaluated mean temperature and temperature variation over time. Mean temperatures and associated standard deviations were also mapped across the study area to determine spatial patterns. The purpose of determining where these stanzas were located in the time series was to provide two time periods between which to compare tunicate frequency of occurrence (FoO) and catch per unit effort (CPUE) to understand if temperature is a driver of tunicate distribution and abundance.

2.4 Tunicate Abundance and Distribution

2.4.1 Frequency of Occurrence and Catch Per Unit Effort Analysis

Understanding where core areas of tunicate presence and abundance are within the study area was important to narrowing down which areas might change over time. In order to understand where consistent “hot spots” were, I used a 3 by 4 grid to divide the entire study area into 12 regions by breaking longitude into three bins (160−165 °W, 165−170°W, and 170−175°W) and latitude into four bins (54−57°N, 57−60°N, 60−63°N, 63−66°N) (Figure 2). Breaking the entire study area into smaller regions of combined stations reduces disparity in sampling effort present at smaller scales. Additionally, this approach allowed for examination of patterns at a larger scale for identification of regional distribution and abundance patterns. Eleven of the twelve regions cover sea area while the last is taken up by land and therefore has no tunicates in it and was excluded from analysis. Frequency of occurrence for each complex was calculated by summing the number of years the taxon was present in that region and dividing by how

many times stations in that region were sampled. (FoO = summed presence in a region/ number of samples in a region). In addition to FoO, mean CPUE for each complex was calculated by averaging CPUE in a particular region.

The goal in calculating FoO and mean CPUE per region was to be able to use both metrics to assess potential differences between the cold and warm temperature stanzas at a regional scale. Differences between stanzas were calculated by comparing the FoO or CPUE in the cold stanza to the FoO or CPUE in the warm stanza.

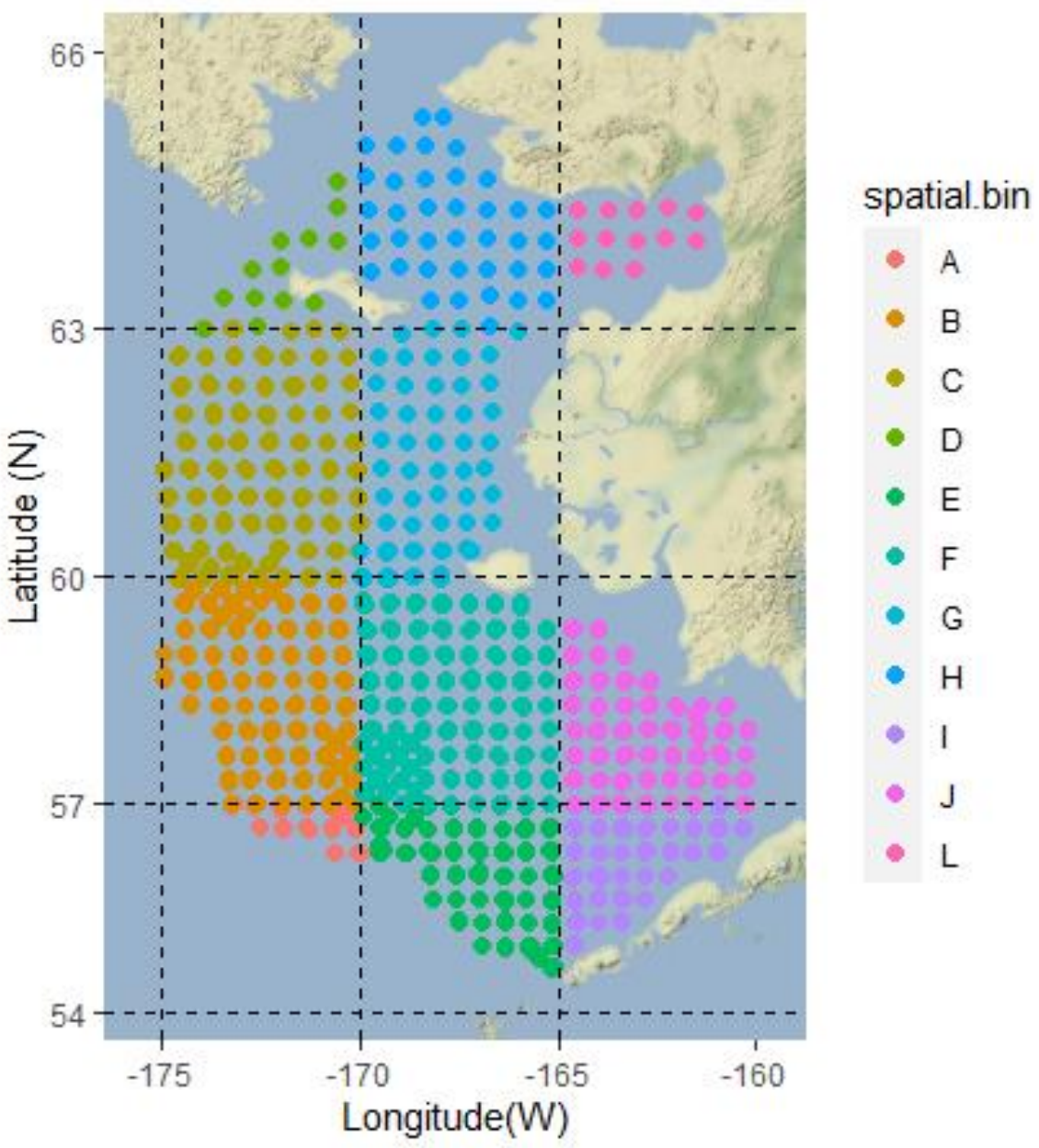

Figure 2: Twelve regions created by averaging all stations in four latitude and three longitude bins for a regional-level analysis. Each dot represents an individual station within the region.

2.5 Linear Models

Simple linear models (lms) were fit for CPUE as a function of bottom temperature and depth (CPUE~ Temperature + Depth) for each species complex as well as all tunicates combined. Model residuals were assessed for violations of model

assumptions, and Akaike Information Criterion (AIC) was used to select the best fit of these models.

2.6 Spatiotemporal Modeling

Preliminary analyses demonstrated changes in temperature over the time series (1987—2019) and across the EBS study area. These temporal and spatial temperature structures may also affect tunicate occurrence and abundance and distribution. While measured variables can be used as predictors in statistical models many of these models cannot incorporate unmeasured, or latent, variables. These latent variables, or inherent variation in “state” not necessarily due to environmental covariates (Kristensen et al 2016), require geostatistical models. To quantify temporal and spatial patterns of tunicate occurrence and abundance patterns and make predictions in areas not explicitly sampled a model that can incorporate spatiotemporal structure is desirable (Anderson et al. 2022).

The R package sdmTMB fits species distribution models using stochastic partial differential equation matrices (SPDE; Commander et al. 2022, Johnson et el. 2021, Ward et al. 2022). SPDEs are equations that execute relations between the partial derivatives of a function with many variables (PDEs) via random force terms and coefficients (Krasinski et al. 2019). First, a mesh is generated using the location data (in this case, latitude and longitude from each station converted to Universal Transverse Mercator (UTM) coordinates. The analyst designates the number of “knots” over which the stations will be reduced, allowing capture of existing species distribution data, and interpolation between stations. For this model, 50 knots were selected over which to interpolate; 80 created too fine a mesh and resulted in interpolation close to existing

field stations and 10 was too coarse, with too much distance between observed data points, which could fail to capture finer-scale changes in distribution. Unique meshes for each species complex, as well as one mesh for all the tunicates combined, were generated to conduct the spatiotemporal analyses because each species complex had an inherently different distribution in the study area.

SPDE approximations to Gaussian Random Fields (random fields involving a generalized one-dimensional normal distribution to higher dimensions) using integrated nested laplace approximation (INLA) can make large spatial models run more quickly and be less computationally exhausting (Commander et al. 2022, Taylor and Diggle 2014, Ward et al. 2022). INLA is a method to approximate Bayesian inference that is popular in spatial statistics due to its analytical speed with large data sets compared to other methods (Taylor and Diggle 2014). The sdmTMB package essentially fits extended generalized linear mixed models (GLMMs) with spatial and spatiotemporal components approximated in the covariance structure as random effects (Ward et al. 2022). Within the modeling framework, spatiotemporal fields can be invoked if one assumes spatial variation is dynamic over a time series or omitted if the spatial variance is expected to be constant (stationary) over time.

The response variables of interest in this study were presence/absence and CPUE of each of the three species complexes as well as all species combined. I generated different classes of sdmTMB models to identify the group that explained the most variability: presence/absence as a function of spatial information, presence/absence as a function of spatial and temporal information, CPUE as a function of spatial information, CPUE as a function of spatial and temporal information

as well as spatiotemporal models with covariates depth and temperature included. All spatiotemporal models (by year) were fit assuming a random walk spatial autocorrelation as I anticipated that both occurrence and abundance of tunicate species at one station was more like the stations nearest than at stations that were further apart. Similarly, I expected tunicate abundance and distribution to be more similar in two consecutive years than in increasingly longer intervals between samples.

Different families and links were used to fit the models dependent upon the data structure. Links are used to connect a model's outcome (random component) to the predictors (systematic component) when data and the model residuals are not normally distributed. All presence/absence models were fit with a binomial family (either 0 or 1) and a logit link while the CPUE models were fit assuming a Tweedie family distribution and a log link. These are the canonical or default links for these distributions. Tweedie was selected for the latter because of the continuous nature of the response variable (CPUE) and large number of zeros in the data.

The R package, sdmTMB, uses Template Model Builder (TMB), a model fitting package for modeling latent variables, to implement maximum likelihood estimation using INLA for random effects associated with space and time (Kristensen et al. 2016). A covariance matrix typically describes the interrelationships of the observational pairs within a statistical model. Here a Matérn covariance matrix is used to model covariance depending on the magnitude of the variability and the shape of the function. This matrix describes the spatiotemporal component underlying the distributions of the taxa.

Model selection was based on a combination of residual plots, comparison with model AICs, visual assessment of maps of observations compared with model

predictions, and sdmTMB's cross-validation function. The latter function performs cross-validation by withholding some model data in iterations or "folds" to see how model predictions change when varying data is retained. It is possible to specify the number of folds in accordance with temporal or spatial patterns to examine for which years or locations the model fails to perform as well; however, I used the sdmTBM cross validation function default of 8 randomly selected folds.

From an extensive list of candidate models (see appendix), the top models were selected comparing the summed omitted log likelihood per fold across all omitted data for candidate models for each species (Anderson et al. 2022). These are the default values for the sdmTMB_cv() function. For log likelihood, better fit is signified by higher values. Additionally, I calculated residual mean squared error, which serves as a standalone measure of model fit. Here, the lower the error the better the model fits the observed data points. RMSE was calculated for each candidate model.

To make predictions across the sample area, a prediction grid was created. I used a 50 km^2 prediction grid by generating sequences of 25 km from the minimum values to the maximum values in both latitude and longitude. I chose 25 km as a meaningful scale for which to obtain predictions based on the station locations for the observed data, the variation in observations across the study area, and the interpolation used to build the model. Predicted estimates of occurrence and abundance were then mapped out across the spatial grid; the error associated with these estimates was also mapped.

3. RESULTS

3.1 Temporal and Spatial Temperature Patterns

Bottom temperature ranged from -2.1 to 15.3−°C during the period of observation. The mean temperature over the entire time series was 2.17−°C with a standard deviation of 2.16−°C. Temperature fluctuated interannually with smaller deviations (on average 1.6 standard deviations) from the mean until about 2005, before the beginning of the cold stanza. Temperature shows a sharp increase by the end of the time series as the warm stanza developed (Figure 3). The years 2005—2010 mark the colder than normal stanza (approx. -1.9 SD from the mean) while 2015—2019 represents a warmer than normal stanza (approx. +2.3 SD from the mean). This aligns with previous findings, confirming the stanzas already noted in the literature (Stevenson and Lauth 2019). While the mean varies by year, it is important to note the pronounced change in variance as well; temperature variability doubles in the warm stanza near the end of the time series compared to the neutral stanza prior to the cold stanza (Figure 3).

In addition to temporal patterns in mean temperature and deviation in temperature from the mean, there are spatial patterns within the Bering Sea (Figure 4). The NBS is warmer (marked by warmer red colors) and more variable (bigger dots) than the EBS. The water is considerably shallower in the NBS than the EBS (mean 50 m, 78 m respectively), especially extending into Norton Sound. The cold pool can visibly be seen as the relatively dark blue elbow shape flanked by purple on either side (Figure 4).

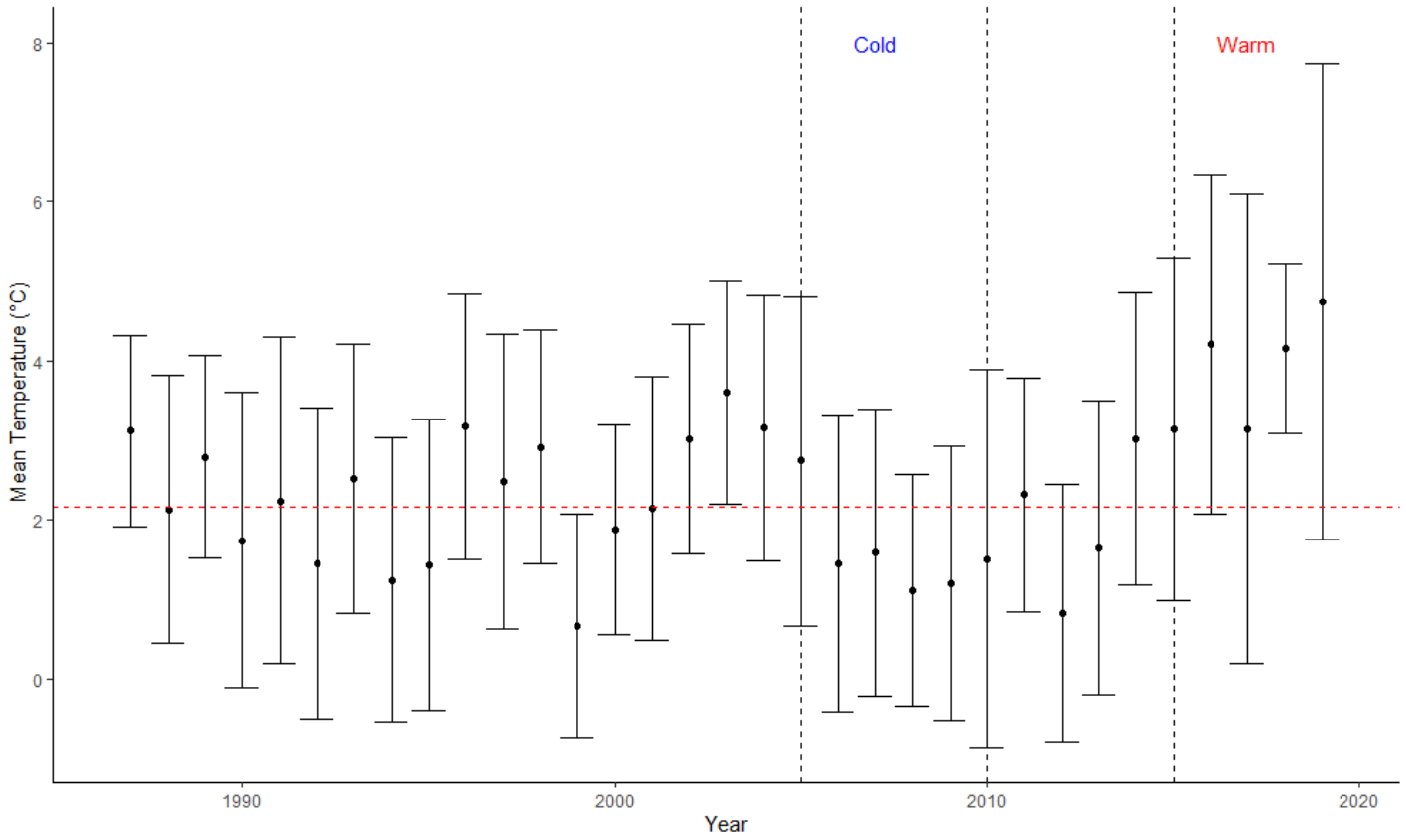

Figure 3: Mean bottom temperature per year across the time series. Error bars represent standard deviation from the mean. The warm and cold stanzas are annotated with labels and dashed lines. The period between the stanzas and prior to the cold stanza is considered neutral. The mean temperature across the time series is 2.17 °C marked with a red dashed line.

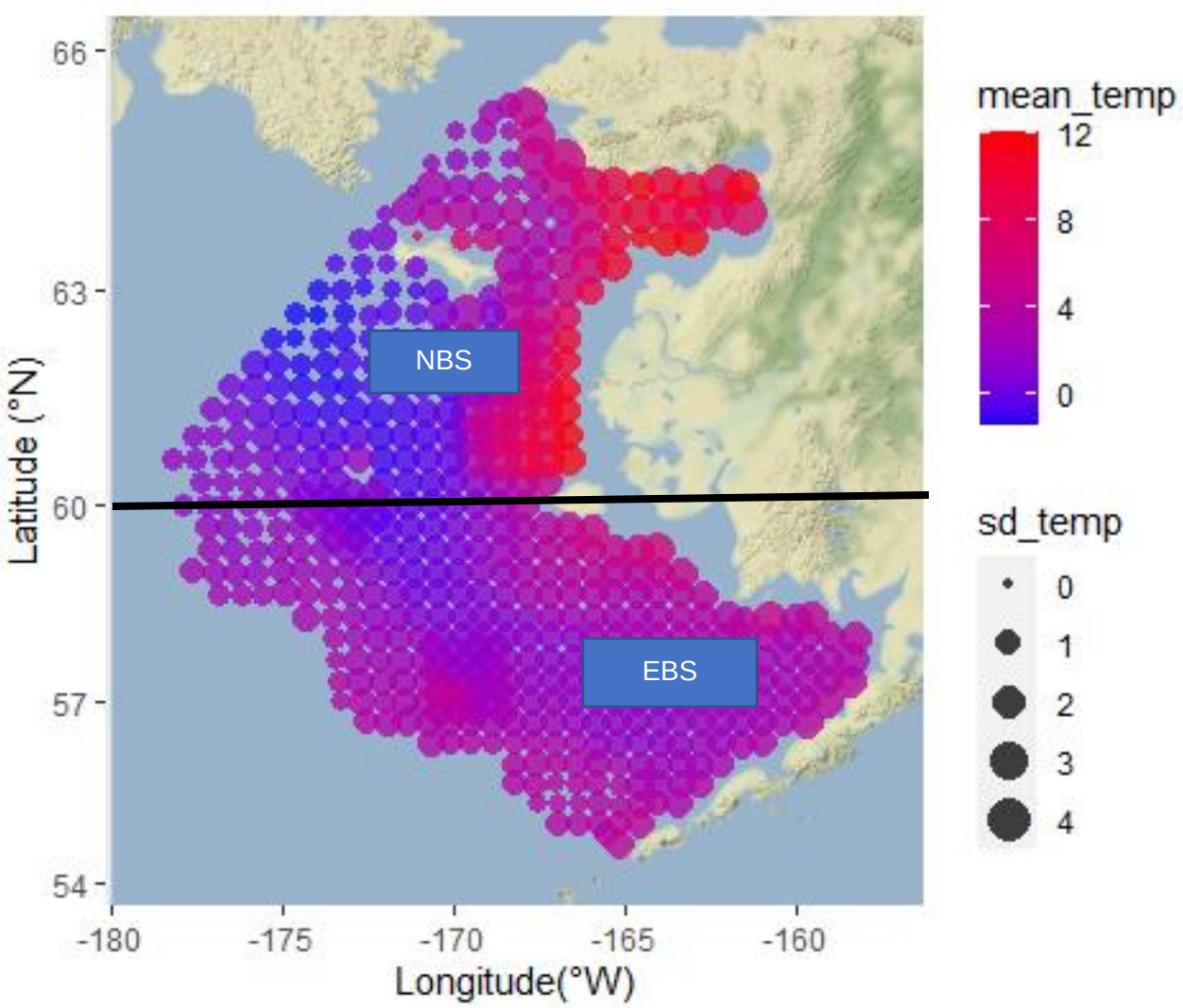

Figure 4: Bottom temperature is on average warmer (red color) and more variable (bigger dots) in the NBS across the entire time series.

3.2 Tunicate Frequency of Occurrence and Catch Per Unit Effort

The three taxa varied in occurrence patterns. *Halocynthia* was the least commonly occurring, only showing up in 31% of the stations (Figure 5). *Boltenia* and *Styela* were each present in about 80% of stations over the time series (not necessarily the same stations). *Styela* appeared to be the least localized, with broad distribution. *Styela* was nearly ubiquitous throughout the study area (Figure 5).

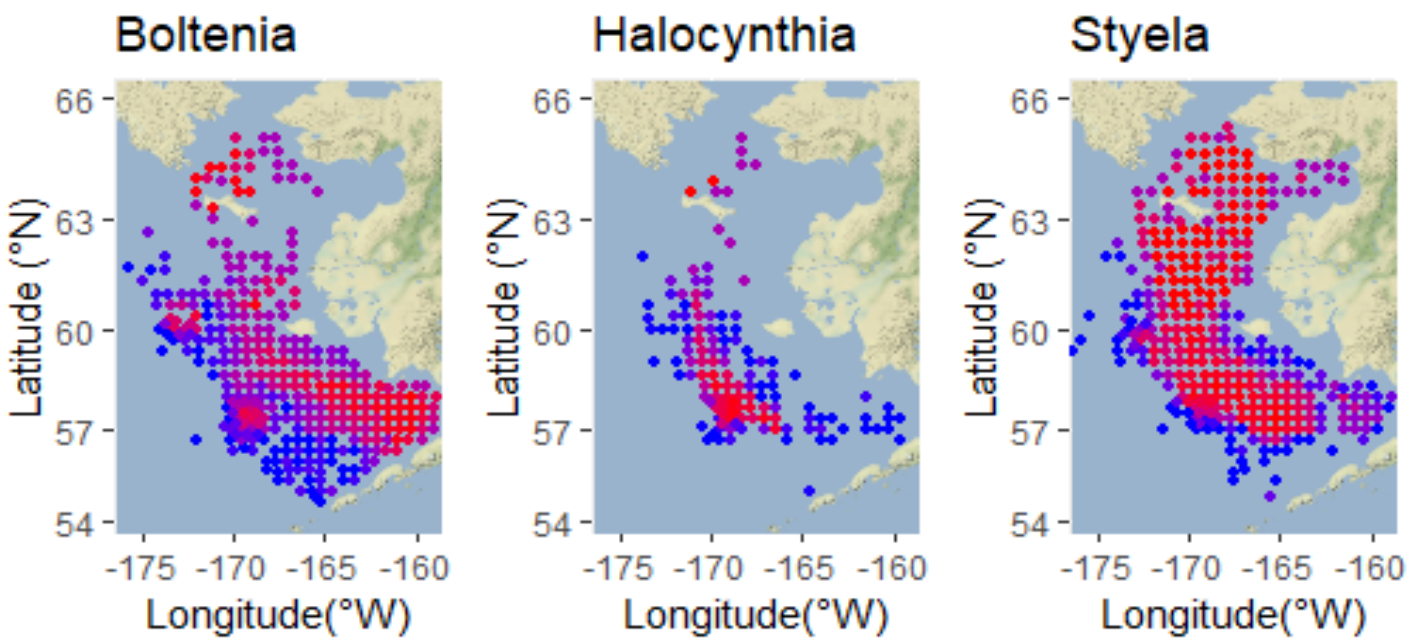

Figure 5: Frequency of occurrence by station for each of the three species complexes over the time series. Red signifies 100% frequency of occurrence at a station and blue indicates that species was found rarely (less than 25%) at that location. Purple dots represent stations where the species is found about half the time.

The mean CPUE per year for all tunicates was 23.5 kg/ha and the mean CPUE per station for all tunicates was 1.49 kg/ ha. Figure 6 shows the interannual variability in temperature with mean tunicate CPUE. Periods of colder and warmer water (the cold and warm stanzas) show associated increases (cold) and decreases (warm) in mean tunicate abundance that are corroborated in Table 1. *Halocynthia* had the most localized distribution, but the highest mean CPUE per year from the early 2000's and on. *Boltenia*, with its intermediate distribution (Figure 5) had the lowest mean CPUE per year by weight (Figure 6a). *Styela* with is the most broadly distributed tunicate spatially but isn't found in as exceptionally high numbers per station as *Halocynthia*.

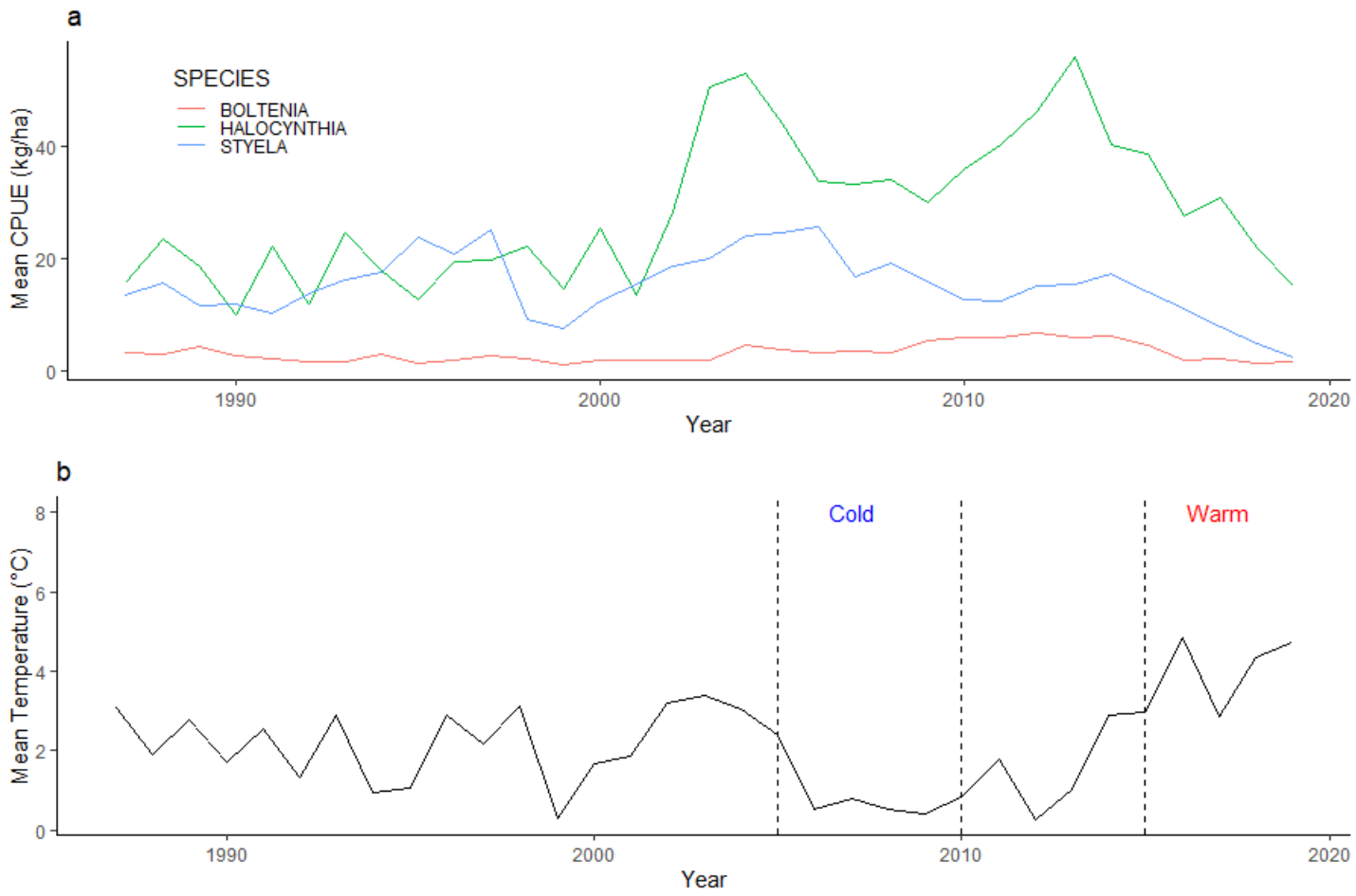

Figure 6: Time series of (a) tunicate catch per unit effort for each year for each of the three species complexes and (b) average bottom temperature by year for the time series.

When tunicate CPUE was compared in the same subset of years in the EBS and NBS, tunicate biomass was generally higher in the EBS than in the NBS. *Halocynthia* dominated the EBS in all three years but was infrequently found in the NBS (Figure 7). Although it was very localized, not occurring broadly, (Figure 5), it was found in very high biomass where it occurred. *Styela* was the most abundant species complex by biomass in the NBS during 2010, 2017, and 2019. In the EBS it had lower CPUE than

Halocynthia, despite being more widely distributed, suggesting it may be less sensitive to water temperature (Figure 6).

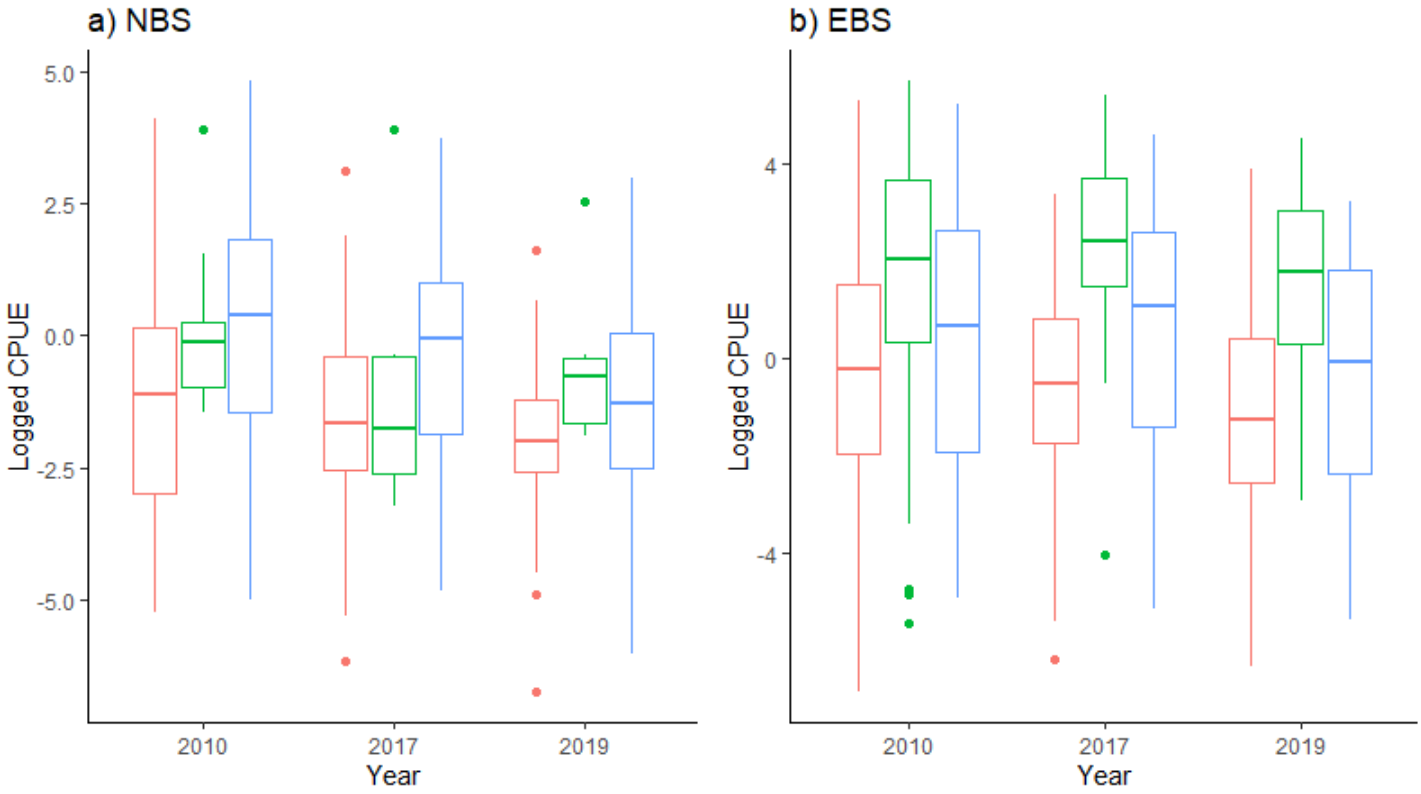

Figure 7: Logged catch per unit effort of a) Northern Bering Sea and b) Eastern Bering Sea for Boltenia (pink), Halocynthia (green), and Styela (blue) for the three years the Northern Bering Sea stations are included in the data.

3.2.1 Tunicate Frequency of Occurrence and Catch Per Unit Effort by Stanza

Boltenia and *Halocynthia* decreased in FoO between the cold and the warm stanzas (Table 1). *Styela* FoO increased slightly between the two stanzas while tunicates combined remained constant (Table 1). *Boltenia*'s largest increase in FoO between the cold and warm stanzas occurred in region G in the EBS. The increase in *Styela* FoO appeared to occur largely in region L in the NBS (Figure 8). *Styela* increases in FoO were larger in magnitude than the other two species.

All three species decreased in average CPUE between the cold and warm stanzas (Table 1). CPUE was on average higher in the cold stanza than the warm, and there tended to be higher variability around this mean in the cold stanza than the warm. Region F experienced increases in CPUE between the cold and warm stanza for all three species even though all three species experienced overall decreases in CPUE between the stanzas. Again, *Styela* differences were largest in magnitude (Figure 9), with 1.692 thousand kg/hectare decline in CPUE (Table 1).

Table 1: Mean frequency of occurrence (as a percentage) and mean catch per unit effort (in kg/ha) in each stanza for each species and the difference between the two. The color shows the direction of the change; blue is a decrease from cold to warm, red is an increase from cold to warm, and black signifies no change.

Species	Metric	Cold Stanza	Warm Stanza	Difference
Bolt	Frequency of occurrence	11%	8%	3%
Bolt	Catch per unit effort	490 kg/ha	100 kg/ha	390 kg/ha
Halo	Frequency of occurrence	3.1%	2.6%	0.5%
Halo	Catch per unit effort	1080 kg/ha	690 kg/ha	390 kg/ha
Sty	Frequency of occurrence	16%	18%	2%
Sty	Catch per unit effort	3000 kg/ha	1308 kg/ha	1690 kg/ha
All	Frequency of occurrence	8.6%	8.6%	0
All	Catch per unit effort	1310 kg/ha	680 kg/ha	630 kg/ha

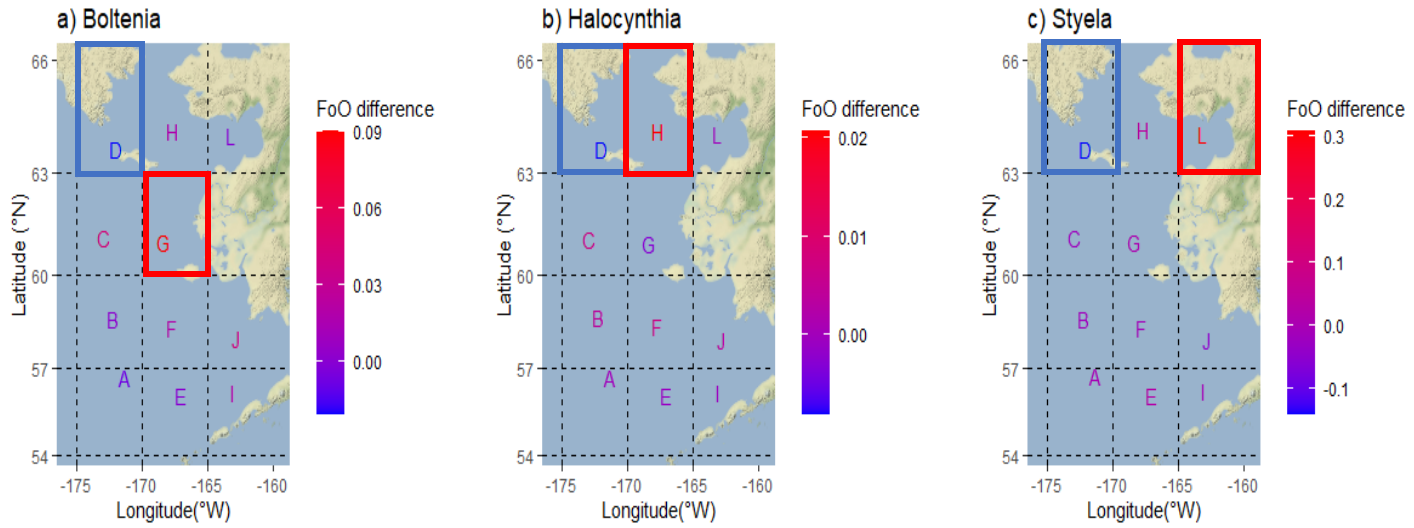

Figure 8: Difference in frequency of occurrence between cold stanza and warm stanza for a) Boltenia, b) Halocynthia, and c) Styela in each of the 12 regions. Most pronounced increases and decreases for each species are outlined in red and blue respectively.

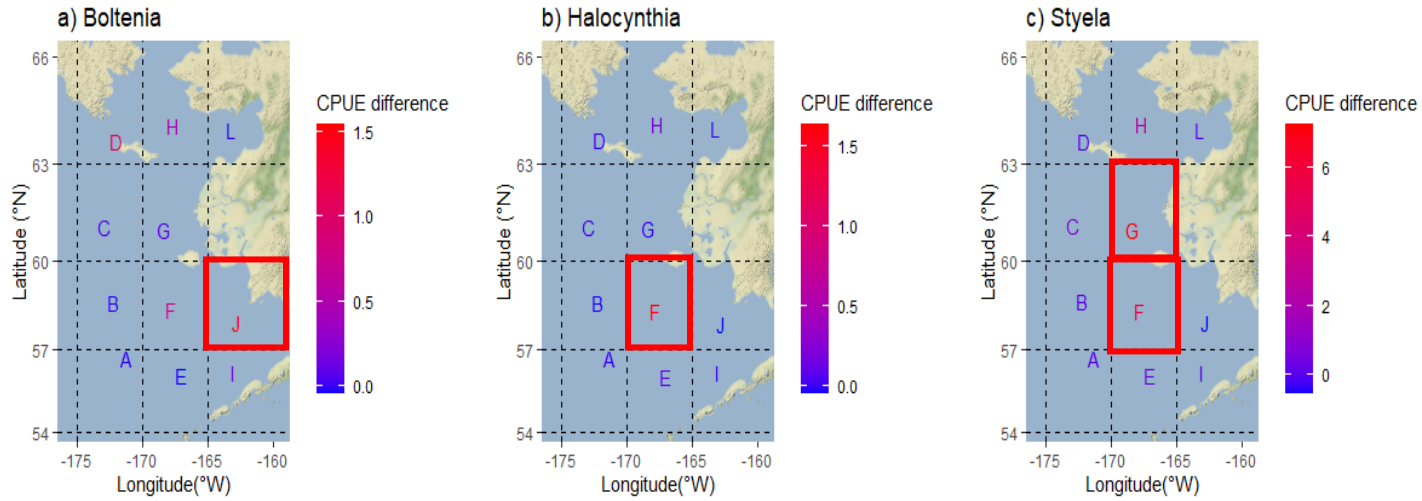

Figure 9: Difference in catch per unit effort between cold stanza and warm stanza for a) Boltenia, b) Halocynthia, and c) Styela in each of the 12 regions. Most pronounced increases for each species are outlined in red.

3.3 Linear Model Results

Temperature and depth were both significant predictors in linear models of CPUE (Table 2) but did not explain much variation in any of the cases. They both appeared to be important structuring variables (slopes significantly different from zero), but residual

error is high with space and time, or other unmeasured variables unaccounted for. These results motivate the use of spatiotemporal SDMs to better understand how spatial arrangement influences distribution over time. *Halocynthia* showed an increase in CPUE with temperature while the others showed decreases (Table 2). CPUE for all complexes increased very slightly with depth (low positive coefficients in Table 2).

Table 2: Summary table for linear models of tunicate catch per unit effort with covariates depth and temperature for all three taxa as well as for all tunicate species combined.

Species	F Stat	P	Adj.R^2	Temp Coef.	Temp SE	Temp P	Depth Coef.	Depth SE	Depth P
Bolt	28.58	<0.001	0.017	-0.05	0.008	<0.001	0.003	0.001	0.01
Halo	27.64	<0.001	0.05	0.1	0.27	<0.001	0.04	0.006	<.001
Sty	46.18	<0.001	0.03	-0.09	0.01	<0.001	0.007	0.002	<.001
All	191.3	<0.001	0.05	-0.07	0.008	<0.001	0.01	0.001	<.001

3.4 Spatiotemporal Model Results

Spatial and spatiotemporal models were fit for each of the three species complexes (*Boltenia*, *Halocynthia*, *Styela*) plus one for all tunicates combined (see full list of models in the appendix). The model results are in Table 3. CPUE for all three tunicate taxa was modeled as a function of spatial information only (no environmental covariates) with 1) assumed constant spatial variation and 2) assumed dynamic spatial variation by year (spatiotemporal, random walk structure). Both models were included for comparison. The last three models for each species are CPUE as a function of bottom temperature to evaluate the impact of temperature once the error associated with spatial and temporal processes is accounted for. Table 3 shows a complete list of models fit.

Table 3: Table showing each species complex, the model number, the structure of the model (spatial only or spatiotemporal), whether the temperature covariate was included in the model, the delta AIC (the lowest AIC value measured from each of the others), the coefficient estimate for the covariate (either space only, space and time together, or temperature) and its associated standard error, and the Matérn distance (estimated distance at which points become independent of each other for a given model). Best fitting models (determined by delta AIC) for each species are bolded. The response variable was catch per unit effort in all cases.

Species	Model	Structure	Covariate	Δ AIC	Coef. Est	Coef. SE	Matérn
Boltenia	1	spatial	none	397	-7.87	1.44	317.10
Boltenia	**2**	**spatiotemporal**	**none**	**0**	**-7.22**	**1.39**	**314.30**
Boltenia	3	spatiotemporal	Temperature	369	-0.04	0.03	313.69
Halocynthia	4	spatial	none	67	-15.57	6.46	541.84
Halocynthia	**5**	**spatiotemporal**	**none**	**0**	**-13.76**	**2.60**	**295.29**
Halocynthia	6	spatiotemporal	Temperature	2	-0.03	0.05	293.01
Styela	7	spatial	none	351	-7.56	2.50	404.66
Styela	8	spatiotemporal	none	12	-7.63	1.84	324.96
Styela	**9**	**spatiotemporal**	**Temperature**	**0**	**-0.11**	**0.03**	**318.44**

3.4.1 Spatial and Spatiotemporal Models

For all three species, the spatiotemporal models were more supported than the spatial models according to AIC. There is also lower standard error around the coefficient for the spatiotemporal models than the spatial models (Table 3). The Matérn distance is based on the distance at which the data points become independent of each other and are not spatially related. It is a helpful metric for interpreting how spatially correlated the points are for a particular species in a particular model. *Boltenia* observations become independent of each other at 314 km² in the best fitting model (Model 2), *Halocynthia* observations become independent of each other at 295 km²

(Model 5). *Halocynthia's* coefficient for spatial (-15.57) and spatiotemporal (-13.76) information are nearly double the size of any other species.

The *Styela* predictions become a bit patchier and more pinpointed when a dynamic spatial variation is assumed (Figures 10c,11c). Boltenia also becomes patchier, especially in the southeast portion of the Bering Sea. Halocynthia spatial predictions don't change much between the spatial and spatiotemporal models. Individually fit species models are more informative than the model fit for all tunicates combined because individual species varied in distribution and abundance and therefore are not included in these results. The patterns in the combined models were largely driven by the most ubiquitous taxon, *Styela*.

.

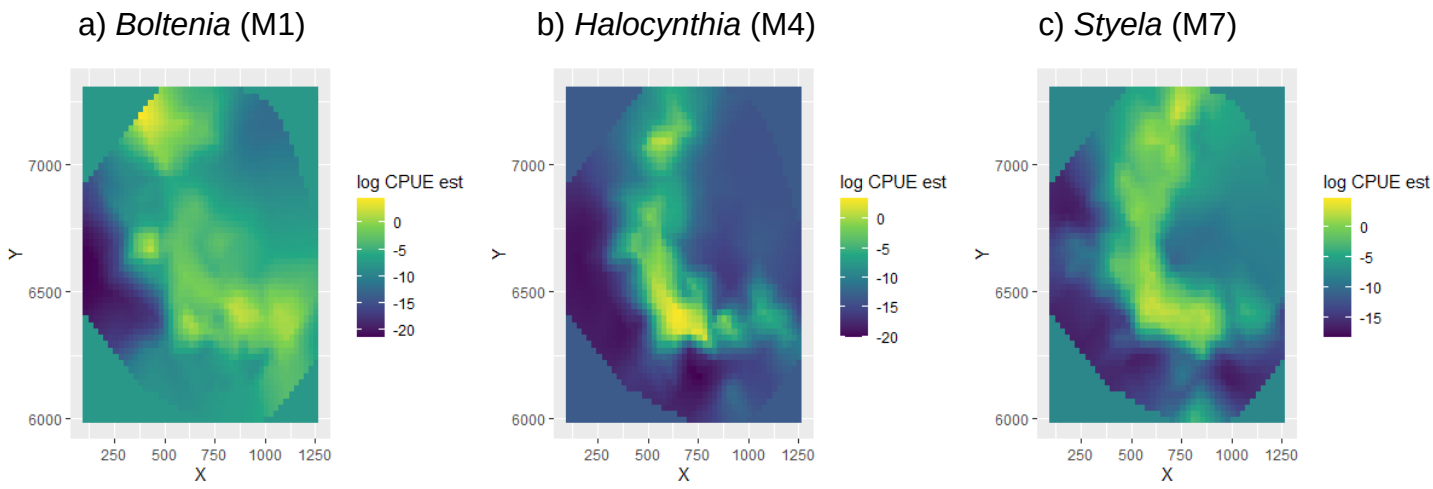

Figure 10: Predictions for catch per unit effort estimates from spatial models for a) Boltenia, b) Halocynthia and c) Styela. Model number corresponds to column 2 in Table 3. X and Y values are Universal Transverse Mercator coordinates. Estimates are log transformed catch per unit effort for ease of visualizing distribution patterns due to high number of zeros in catch per unit effort data. Note varying scales for each species.

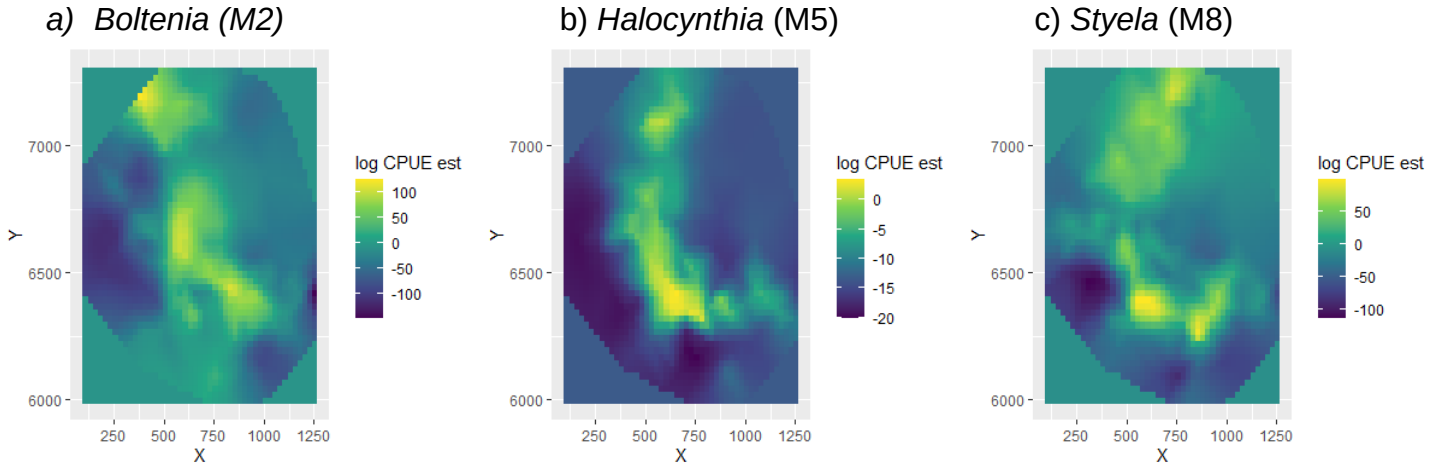

Figure 11: Predictions for catch per unit effort estimates from spatiotemporal models for a) Boltenia, b) Halocynthia and c) Styela. Model numbers correspond to column 2 in Table 3. X and Y values are Universal Transverse Mercator coordinates. Estimates are log transformed catch per unit effort for ease of visualizing distribution patterns due to high number of zeros in catch per unit effort data. Note varying scales for each species.

3.4.2 Spatiotemporal Models with Environmental Covariates

Temperature

When included as a covariate in the spatiotemporal models, temperature had a weaker relationship with CPUE than spatial information alone as shown by a coefficient of smaller magnitude. Temperature does not influence spatial predictions for *Boltenia* and *Styela* (Figures 11a-b, 12a-b) but does appear to contribute to explaining variance in the data (Table 3). Of the three species complexes, *Halocynthia* predictions change the most when temperature is included as a covariate, with regions of high abundance becoming more localized than when the temperature covariate is omitted (Figure 12b). All coefficients show negative effects on CPUE with temperature (Table 3). *Styela's* coefficient shows the largest decrease in CPUE (-0.11) with temperature compared to the other two species (-0.04, -0.03; Table 3). *Styela* is the only species for which a model with temperature included as a covariate is preferred over a model without the covariate (Table 3), although the output for *Halocynthia* shows support for including temperature in the model (ΔAIC-2). *Styela* observations become independent of each other at 318 km^2 (Model 9).

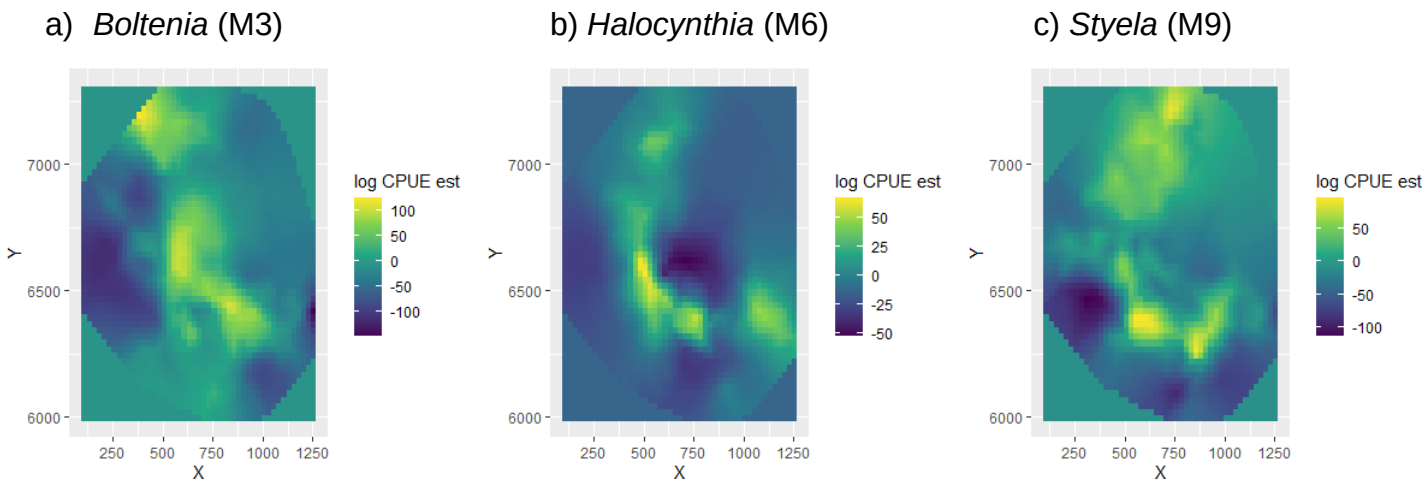

Figure 12: Predictions for catch per unit effort estimates from spatiotemporal models with temperature as a covariate for a) Boltenia, b) Halocynthia and c) Styela. Model numbers correspond to column 2 in Table 3. X and Y values are Universal Transverse Mercator coordinates. Estimates are log transformed catch per unit effort for ease of visualizing distribution patterns due to high number of zeros in catch per unit effort data. Note varying scales for each species.

Depth

The spatiotemporal models do not support a direct relationship between depth and tunicate abundance. The coefficient for depth is not significantly different from 0, and the AIC score increases when depth is added to models.

3.4.3 Model Validation

The summed log likelihood values corroborated AIC in model selection from the candidate list; the values were highest for the *Boltenia* and *Halocynthia* spatiotemporal models without environmental covariates and highest for *Styela* with temperature included as a covariate. RMSEs were calculated for the spatiotemporal models (with and without temperature included as a covariate) as an additional measure of fit. Halocynthia had the smallest RMSE (15, 18 for models with and without covariates respectively) While Boltenia had the highest (RMSE = 33 for all models). As these values can range from 0 to infinity, all three of the species represent quite good fit (low

RMSE), although RMSE is known to be biased in models of this complexity (Anderson et al. 2022).

3.4.4 Indices of Abundance

Using the spatiotemporal model (no covariates) developed for each species, predicted CPUE trends for all three species, and all tunicates combined, show similar trends over the time series, but responses vary in magnitude (Figure 13). *Styela* predictions are higher than the other two tunicate species in the dataset, perhaps reflecting the broader distribution of this species in the study area. In general, 2010 was a year of particularly high tunicate abundance, although the mid-2000s also showed high CPUE predictions for *Styela* that were not observed in the observed annual averages (Figure 6).The declines seen in 2019 represent a return to baseline numbers seen near the beginning of the time series during a period of higher interannual variation of temperature for *Halocynthia* and *Boltenia,* although their trends in subsequent years is unknown given the lack of data. The prediction trend (black line) for all tunicates combined looks to be mostly driven by peaks and troughs in *Styela* which is the most abundant species from the estimates.

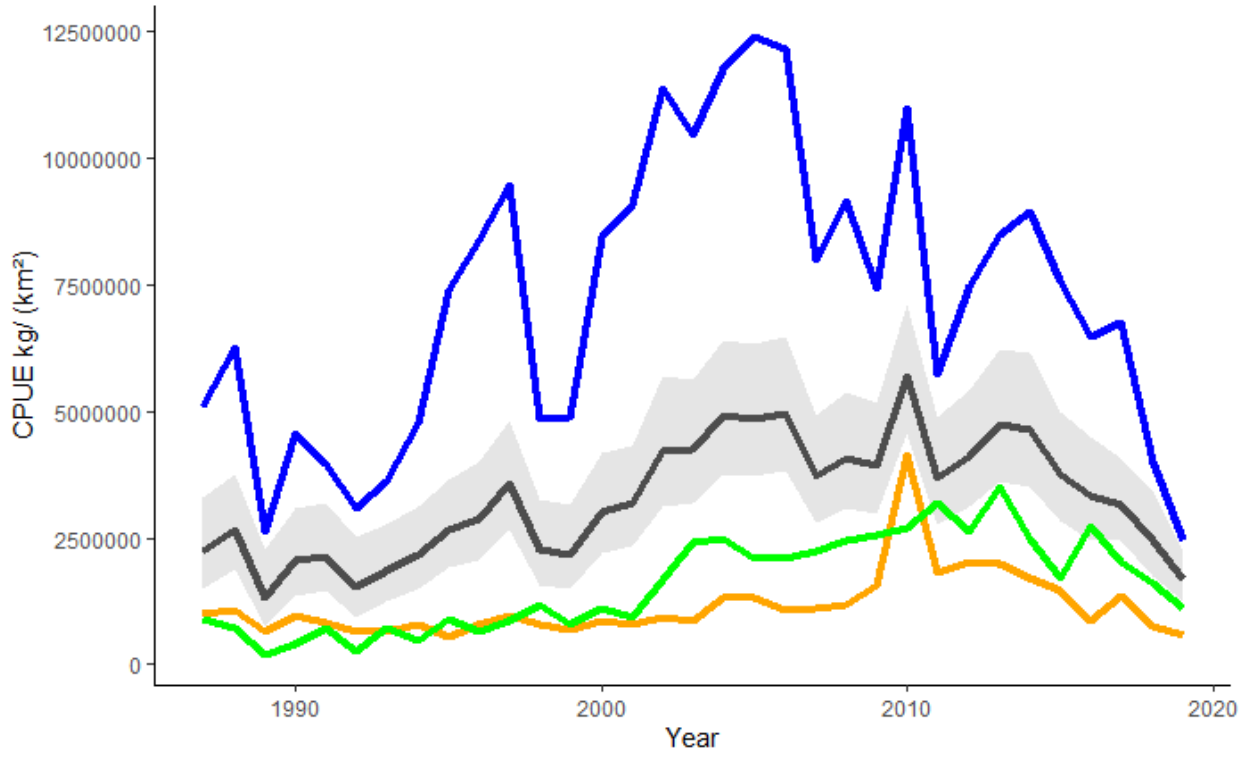

Figure 13: Catch per unit effort (in kg/ km²) predictions generated for Boltenia (orange), Halocynthia (green), Styela (blue) and all tunicates combined (black) with associated standard error (grey). The predictions are from spatiotemporal models for all three species without environmental covariates.

4. DISCUSSION

Spatial and Temporal Patterns are Primary Drivers of Tunicate Abundance

Spatiotemporal models were an improvement over spatial models alone and temperature explained additional variance. Regional-level changes in frequency of occurrence and catch per unit effort do not necessarily align with the overall decreases seen when data are considered in aggregate across the Bering Sea, suggesting the importance of geography in determining distributions. For example, all three tunicate species experienced an increase in mean CPUE in region F between the two stanzas although the overall trend in CPUE across all regions was a decline (Figure 9). Region

F is in the center of the EBS, where the average depth is 52.5 m; additionally, Region F is located within the cold pool. This location may contribute to increased CPUE here while decreases occur elsewhere in the presence of warming temperatures; the cold pool may represent a pocket of reprieve in an otherwise warming environment. This result also supports the importance of temporal information in species distribution models, as the location and extent of the cold pool changes annually and at longer scales, and we know the cold pool is shrinking with warmer temperatures over time. The fact that regional-level results do not mirror overall CPUE trends speaks to the importance of including measures of spatial and temporal variation in predicting tunicate abundances and distributions in an area as big as the Bering Sea, despite its homogenous bathymetry. Although depth was a significant factor in linear models, it did not explain additional variance once the spatial and temporal variance structure were accounted for. This is likely due to the depth structure in the Bering Sea; there is no continuous slope or depth gradient along which to test the importance of depth to these communities, but rather a simple bathymetry where other factors are likely stronger structuring variables.

Tunicates are More Abundant in Colder Environments

Frequency of occurrence was higher in the cold stanza for two of the three species analyzed and mean catch per unit effort was higher during the cold stanza for all three species. All three species demonstrate predicted increases in CPUE in 2010 at the end of the cold stanza and sharp declines in 2019 at the end of the warm stanza in the model-generated index of abundance. There is higher variability in both FoO and CPUE

in the cold stanza than the warm stanza, suggesting that when conditions are more suitable (colder) tunicates have the capacity to increase substantially in both distribution and biomass, but when conditions are less suitable (warmer), the observed CPUE declines along with spatial distribution, and the index of abundance hovers closer to the long-term mean.

Cold and Warm Stanzas Drive Occurrence and Abundance in a Regional-Level Analysis

Changes in FoO occurred in more regions than did CPUE. Thus, FoO may be more responsive to temperature, but these changes in FoO are not visible until local populations have been significantly changed. CPUE is likely an earlier indicator of change in response to temperature due to the continuous nature of the variable and the fact that abundances are likely to decline in CPUE before ceasing to be present. The largest increases and decreases in FoO between the cold and the warm stanzas for most species occurred in the Northern Bering Sea where temperatures are known to be increasing more rapidly. It is worth keeping in mind that there are smaller sample sizes in the NBS. While this doesn't affect comparisons between the NBS regions (D,H,L) and the rest of the regions due to mean per region calculations, the NBS data contains both the coldest (2010) and the warmest (2019) year in the time series, possibly impacting comparisons between the two stanzas in Northern Bering Sea regions D, H, and L. NBS data also includes an uneven number of cold (1 year, 2010) and warm years (2 years, 2017 and 2019).

Spatiotemporal Models Enabled Description of Spatial and Temporal Patterns in Tunicate Abundance

This dataset is unique in the extent of both spatial and temporal information that it includes, lending to the use of more advanced modeling techniques. Most datasets either cover a spatial zone in one year, or the same site over time; very infrequently do environmental datasets contain both spatial and temporal data collected at this extent. The high quality of the data provided the opportunity to explore a cutting-edge modeling technique and assess its effectiveness in predicting tunicate abundances and distributions for the purpose of identifying indicators of environmental change in the Bering Sea.

The models fit the observed data well based on visual assessments of the observations compared to the predictions and were further validated with cross validation methods inherent within the modeling package. The fact that latent variation in space and time is the strongest predictor of tunicate CPUE does not mean that environmental covariates are not important, but that the way these covariates impact CPUE will change over time and across space. Additional covariates that were not measured in this study (e.g., organic matter availability in the benthos, salinity, seasonally averaged surface temperature, bottom type) may be important in further explaining distribution and abundance for these species.

There are many other applications for spatiotemporal models in fisheries management such as to reduce bycatch and manage fisheries more selectively (Dunn et al. 2011), identify changes in populations, manage ecosystems, conserve habitat, and assess effects of climate change (Thorson 2019), and evaluate length-weight

relationships over time that may be influenced by spatial and/or temporal processes (Al Nahdi et al. 2016). Using multivariate spatiotemporal SDMs such as Vector Autoregressive Spatio-Temporal model (VAST) could expand the utility of my analysis further by considering all species complexes within the same multivariate model framework rather than fitting three different models as done in this study.

Tunicate Species Respond Differently to Temperature

Given that different parts of the Bering Sea are experiencing different conditions as climate change progresses, it is not surprising that organisms with variable distributions will not be uniformly impacted by temperature. Predictions of *Halocynthia* CPUE change the most spatially when temperature is included in the spatiotemporal model. They also occupy the smallest spatial area in the Bering Sea of all species complexes examined, which is further cause for concern if their center of distribution is experiencing sustained warming. The spatiotemporal model including temperature as a covariate fit slightly better for *Styela,* suggesting that temperature may be a factor in *Styela*'s distribution and northward movement. *Styela* mean CPUE decreases the most by weight between the cold and the warm stanzas, but the FoO actually increases between the two stanzas. Paired with the fact that *Styela* is the most numerous tunicate species in the NBS, this suggests that an increase in FoO could be driven by higher rates of occurrence in the NBS as the temperature increases in their existing range. The range of the species is increasing though overall biomass is not. Reduced cold pool extent affects phytoplankton production (both timing and magnitude) in the NBS, which decreases organic matter (OM) supply to tunicates in the benthos (Lovvorn et al. 2016).

This may constrain tunicate abundance in the NBS under warming conditions (reduced cold pool extent). Increasing tunicate range northward is also possibly countered by predation from fish or mobile invertebrate species whose ranges are also expanding northward due to warming in the EBS, preventing overall CPUE increases. This seems unlikely to be the main reason for decline as many tunicates have evolved chemical deterrents to predation by fish in addition to their already tough tunic exterior (Holland 2016).

A Suite of Individual Species or "Composite" Indicator May be Most Informative Predictor

The fact that these three tunicate species complexes are not responding to environmental conditions in the same way or by the same order of magnitude suggests that they possess differences in life-history and/or thermal tolerance, possibly caused by adaptation to slightly different temperature conditions. These species do all meet one criterion that has been identified for choosing an indicator species, in that their selection would be based on a sound, quantitative database from the focal region (Carignan and Villard 2002). Multi-species indicators (MSI) are gaining traction in usefulness in monitoring biodiversity (Soldaat et al. 2017) due to an increased robustness to the fluctuations of individual species. Each species essentially serves as a replicate. If consistent trends are observed, it can be inferred that they are indicating similar environmental conditions the same way.

. These three tunicate species represent different levels of abundance within their distribution in the EBS and NBS from patchy (*Halocynthia*), to relatively uniform (*Styela*)

and intermediate abundance and distributions (*Boltenia*). There are examples of commonly encountered species responding more strongly to disturbance than rare species (Koch et al. 2011) as well as rarer at-risk species performing well as an indicator group (Lawler et el. 2003). Abundant and rare species may respond differently to climate extremes (Chen et al. 2020) providing further motivation for including both in a composite indicator complex. This study suggests that tunicates could be useful indicators of shifting climate in the Bering Sea when analyzed in concert. Temperature is clearly related to *Boltenia*, *Halocynthia*, and *Styela* frequency of occurrence and catch per unit effort as shown by the regional analyses and model results in this study, which is the first step in determining whether they will be useful as indicators of climate effects.

Dynamic factor analysis (DFA) is a technique that is used to detect patterns in a set of time series. DFA was used to relate trends in lobster abundance to environmental variables to better predict how at-risk populations will respond to changes in environmental variables (Zuur et al. 2003). This type of analysis would be useful to determine which environmental factors Bering Sea tunicate CPUE is most related to as a possible extension to a multi-species indicator analysis.

Modeling Framework could be Expanded

Sessile invertebrates are important ecosystem engineers playing a part in marine biogeochemistry and moving carbon back to the water column through predation (Hiddink et al. 2014). Because they can't move as adults, and like all marine ectotherms are more vulnerable to temperature shifts than terrestrial counterparts (Hiddink et al. 2014), they are especially susceptible to negative impacts of sustained temperature

increases. Sessile invertebrates lose predator-free space quickly in the intertidal zone in response to warming water creating thermal mismatches (Harley 2011). The loss of cold pool extent in the Bering Sea could create a similar mismatch between species as sub-arctic species like Walleye Pollock are no longer excluded from areas historically too cold for them much of the year. A study from the tropics showed the impacts of storm activity (expected to increase in occurrence and severity with climate change) on sessile invertebrate assemblages in the Great Barrier Reef (Walker et al. 2008). Storms are expected to increase in the EBS and NBS due to loss of sea ice and warming water (Overland and Pease 1982). Large storms in the Bering Sea stir the sediment down to great depths (McConnaughey and Syrjala 2014), possibly impacting invertebrate populations through upheaval and/or siltation from resettling sediment if these events become increasingly common. Mixing water masses due to these storms will also break down the cold pool earlier in the year, possibly creating a positive feedback loop of further warming (Stabeno et al. 2007). For these reasons, historically under-studied and non-economically important sessile invertebrates across the globe may serve as indicators of climate change impacts based on reduced abundance or distribution shifts—either within an intertidal zone or across latitudinal gradients.

Spatiotemporal models may be improved by including seasonally averaged surface temperature instead of the bottom temperatures recorded at the time of data collection, which offer a snapshot, but not an integrated picture of the environment. More work needs to be done on the historically under-studied NBS as climate change continues to change the Bering Sea, causing species (and potentially trawl effort) to move further north.

5. CONCLUSION

Both tunicate abundance and distribution are related to periods of cooler than average and warmer than average temperatures. Latent spatial and temporal correlation explains the largest portion of variability in catch per unit effort. The three taxa in this study were not impacted the same way, indicating different adaptations and tolerances to a broader suite of habitat conditions, suggesting they may have different utilities as environmental indicators. *Halocynthia* may be useful due to its relatively small center of distribution. *Boltenia* may be a useful indicator because it is more widely distributed than *Halocynthia*, but less abundant. Both could be considered “rare” species in terms of distribution (*Halocynthia*) or overall CPUE (*Boltenia*). There are some challenges associated with monitoring rare versus common species which is the focus of recent spatiotemporal model application (Balbuena et al. 2021). *Styela* is an example of a very commonly encountered species which might make it a useful indicator species.

It is also possible that the varying “catchability” of these tunicate species, or ability of researchers to accurately collect all species they trawl over, impacts what we can observe as catch per unit effort data. *Boltenia* can be the most difficult to catch as the stalks they grow from can get tangled in trawl nets (L. Britt, NOAA RACE division, personal communication, November 2022). This means there may be more *Boltenia* out there than we are able to assess with current methods. Understanding how each species will be affected by changing climate may aid in predicting similar responses in other animals. Multivariate models such as VAST could also be a potential route for improving benthic invertebrate species distribution estimates.

6. REFERENCES

Alaska | NOAAFisheries https://www.fisheries.noaa.gov/region/alaska.2022, August 26

Al Nahdi, A., C. Garcia de Leaniz, and A. J. King. 2016. Spatio-Temporal Variation in Length-Weight Relationships and Condition of the Ribbonfish Trichiurus lepturus (Linnaeus, 1758): Implications for Fisheries Management. *PloS One* **11**:e0161989.

Anderson, S.C., E.J. Ward, P.A. English, L.A.K. Barnett. 2022. sdmTMB: an R package for fast, flexible, and user-friendly generalized linear mixed effects models with spatial and spatiotemporal random fields. *bioRxiv* .485545

Balbuena, J. A., C. Monlleó-Borrull, C. Llopis-Belenguer, I. Blasco-Costa, V. L. Sarabeev, and S. Morand. 2021. Fuzzy quantification of common and rare species in ecological communities (FuzzyQ). *Methods in Ecology and Evolution* **12**:1070–1079.

Barnett, L. A. K., E. J. Ward, and S. C. Anderson. 2021. Improving estimates of species distribution change by incorporating local trends. *Ecography* **44**:427–439.

Burgos, J., L. Buhl-Mortensen, P. Buhl-Mortensen, S. Olafsdottir, P. Steingrund, S. Ragnarsson, and Ø. Skagseth. 2020. Predicting the Distribution of Indicator Taxa of Vulnerable Marine Ecosystems in the Arctic and Sub-arctic Waters of the Nordic Seas. *Frontiers in Marine Science* **7**: 1-25

Carignan, V., and M.-A. Villard. 2002. Selecting Indicator Species to Monitor Ecological Integrity: A Review. *Environmental Monitoring and Assessment* **78**:45–61.

Chen, G., W. Wang, Y. Zhang, Y. Liu, X. Gu, X. Shi, and M. Wang. 2020. Abundant and rare species may invoke different assembly processes in response to climate extremes: Implications for biodiversity conservation. *Ecological Indicators* **117**:106716.

Clark, J. B., and A. Mannino. 2022. The Impacts of Freshwater Input and Surface Wind Velocity on the Strength and Extent of a Large High Latitude River Plume. *Frontiers in Marine Science* **8**: 793217.

Clement, J., W. Maslowski, L. Cooper, J. Grebmeier, and W. Walczowski. 2005. Ocean circulation and exchanges through the northern Bering Sea—1979–2001 model results.*Deep Sea Research Part II Topical Studies in Oceanography* **52**(24):3509-3540

Clements, C. F., J. L. Blanchard, K. L. Nash, M. A. Hindell, and A. Ozgul. 2017. Body size shifts and early warning signals precede the historic collapse of whale stocks. *Nature Ecology & Evolution* **1**:1–6.

Commander, C. J. C., L. A. K. Barnett, E. J. Ward, S. C. Anderson, and T. E. Essington. 2022. The shadow model: how and why small choices in spatially explicit species distribution models affect predictions. *PeerJ* **10**:e12783.

Durbin J., and S. J. Koopman. 2012. *Time Series Analysis by State Space Methods*. 2nd ed.

Oxford: Oxford University Press

Dunn, D., A. Boustany, and P. Halpin. 2011. Spatio-temporal management of fisheries to reduce by-catch and increase fishing selectivity. *Fish and Fisheries* **12**:110–119.

Elith, J., and J. R. Leathwick. 2009. Species Distribution Models: Ecological Explanation and Prediction Across Space and Time. review-article, *Annual Reviews*. **40**:677–97

Essington, T. E., S. C. Anderson, L. A. K. Barnett, H. M. Berger, S. A. Siedlecki, and E. J. Ward. 2022. Advancing statistical models to reveal the effect of dissolved oxygen on the spatial distribution of marine taxa using thresholds and a physiologically based index. *Ecography*. **2022:**e06249.

Evans, R., P. A. English, S. C. Anderson, S. Gauthier, and C. L. K. Robinson. 2021. Factors affecting the seasonal distribution and biomass of *E. pacifica* and *T. spinifera* along the Pacific coast of Canada: A spatiotemporal modelling approach. *PLOS ONE* **16**:e0249818.

Francis, F., K. Filbee-dexter, and R. Scheibling. 2014. Stalked tunicates *Boltenia ovifera* form biogenic habitat in the rocky subtidal zone of Nova Scotia. *Marine Biology* **161**:1375–1383.

Froeschke, J. T., and B. F. Froeschke. 2016. Two-Stage Boosted Regression Tree Model to Characterize Southern Flounder Distribution in Texas Estuaries at Varying Population Sizes. *Marine and Coastal Fisheries*. **8**:222-231

Ferrero, L., N. Servetto, J. Laudien, and R. Sahade. 2019. Reproductive biology of the ascidians *Styela rustica* and *Halocynthia pyriformis* from Kongsfjorden, Svalbard, Arctic. *Polar Biology* **42**:1899–1909.

Free, C., J. Thorson, M. Pinsky, K. Oken, J. Wiedenmann, and O. Jensen. 2019. Impacts of historical warming on marine fisheries production. *Science* **363**:979–983.

Grebmeier, J. M. 2006. A Major Ecosystem Shift in the Northern Bering Sea. *Science* **311**:1461–1464.

Harley, C. D. G. 2011. Climate Change, Keystone Predation, and Biodiversity Loss. *Science*.**334**:1124-1127

Hiddink, J., M. Burrows, and J. Molinos. 2014. Temperature tracking by North Sea benthic invertebrates in response to climate change. *Global Change Biology* **21**.117-129.

Holland, L. Z. 2016. Tunicates. *Current Biology* **26**:R146–R152.

Johnson, K. F., N. F. S. Center, E. J. Ward, and N. F. S. Center. 2021. Proposal for the methodological review of sdmTMB for index standardization.

Karp, M. A., S. Brodie, J. A. Smith, K. Richerson, R. L. Selden, O. R. Liu, B. A. Muhling, J. F. Samhouri, L. A. K. Barnett, E. L. Hazen, D. Ovando, J. Fiechter, M. G. Jacox, and M.

Pozo Buil. 2022. Projecting species distributions using fishery-dependent data. *Fish and Fisheries*.

Koch, A. J., M. C. Drever, and K. Martin. 2011. The efficacy of common species as indicators: avian responses to disturbance in British Columbia, Canada. *Biodiversity and Conservation* **20**:3555–3575.

Krainski, E., V. Gómez-Rubio, H. Bakka, A. Lenzi, D. Castro-Camilo, D. Simpson, F. Lindgren, and H. Rue. 2019. Advanced Spatial Modeling with Stochastic Partial Differential Equations Using R and INLA. CRC Press.

Kristensen, K., Nielsen, A., Berg, C. W., Skaug, H. J., & Bell, B. 2016. TMB: Automatic differentiation and laplace approximation. *Journal of Statistical Software*, **70(5)**: 1-21.

Lambert, G., R. Karney, W. Rhee, and M. Carman. 2016. Wild and cultured edible tunicates: a review. Management of Biological Invasions **7**:59–66.

Lawler, J. J., D. White, J. C. Sifneos, and L. L. Master. 2003. Rare Species and the Use of Indicator Groups for Conservation Planning. *Conservation Biology* **17**:875–882.

Lemaire, P., and J. Piette. 2015. Tunicates: exploring the seashores and roaming the open ocean. A tribute to Thomas Huxley. *Open Biology* **5**:150053.

Lin, H., K. Liu, J. Wang, Y. Huang, Z. Li, J. Lin, X. He, S. Zhang, J. Mou, Y. Wang, and B. Xing. 2018. Spatial pattern of macrobenthic communities along a shelf-slope-basin transect across the Bering Sea. *Acta Oceanologica Sinica* **37**:72–81.

Lovvorn, J. R., C. A. North, J. M. Kolts, J. M. Grebmeier, L. W. Cooper, and X. Cui. 2016. Projecting the effects of climate-driven changes in organic matter supply on benthic food webs in the northern Bering Sea. *Marine Ecology Progress Series* **548**:11–30.

Marshall, J., K. C. Armour, J. R. Scott, Y. Kostov, U. Hausmann, D. Ferreira, T. G. Shepherd, and C. M. Bitz. 2014. The ocean's role in polar climate change: asymmetric Arctic and Antarctic responses to greenhouse gas and ozone forcing. *Philosophical Transactions of the Royal Society A: Mathematical, Physical and Engineering Sciences* **372:**20130040.

McConnaughey, R. A., and S. E. Syrjala. 2014. Short-term effects of bottom trawling and a storm event on soft-bottom benthos in the eastern Bering Sea. *ICES Journal of Marine* Science **71:**2469–2483.

Morley, J. W., R. L. Selden, R. J. Latour, T. L. Frölicher, R. J. Seagraves, and M. L. Pinsky. 2018. Projecting shifts in thermal habitat for 686 species on the North American continental shelf. *PloS one* **13**:e0196127.

Nadtochy, V. A., N. V. Kolpakov, and I. A. Korneichuk. 2017. The Distribution of Macrozoobenthos Taxa as Potential Indicators of Vulnerable Marine Ecosystems in the Western Bering Sea: 1. Anadyr Bay Area. *Russian Journal of Marine Biology* **43**:555–567.

Overland, J. E., and C. H. Pease. 1982. Cyclone Climatology of the Bering Sea and Its Relation to Sea Ice Extent. *Monthly Weather Review* **110**:5–13.

Pettitt-Wade, H., T. Pearce, D. Kuptana, C. P. Gallagher, K. Scharffenberg, E. V. Lea, N. E. Hussey, and L. L. Loseto. 2020. Inuit observations of a Tunicata bloom unusual for the Amundsen Gulf, western Canadian Arctic. *Arctic Science* **6**:12.

Pinsky, M. L., A. M. Eikeset, D. J. McCauley, J. L. Payne, and J. M. Sunday. 2019. Greater vulnerability to warming of marine versus terrestrial ectotherms. *Nature* **569**:108–111.

Shenkar, N., and B. J. Swalla. 2011. Global Diversity of Ascidiacea. *PLOS ONE* **6:**20657.

Soldaat, L. L., J. Pannekoek, R. J. T. Verweij, C. A. M. van Turnhout, and A. J. van Strien. 2017. A Monte Carlo method to account for sampling error in multi-species indicators. *Ecological Indicators* **81**:340–347.

Spies, I., K. M. Gruenthal, D. P. Drinan, A. B. Hollowed, D. E. Stevenson, C. M. Tarpey, and L. Hauser. 2020. Genetic evidence of a northward range expansion in the eastern Bering Sea stock of Pacific cod. *Evolutionary Applications* **13:**362–375.

Stabeno, P. J., N. A. Bond, and S. A. Salo. 2007. On the recent warming of the southeastern Bering Sea shelf. *Deep Sea Research Part II: Topical Studies in Oceanography* **54:**2599–2618.

Stabeno, P. J., and S. W. Bell. 2019. Extreme Conditions in the Bering Sea (2017–2018): Record-Breaking Low Sea-Ice Extent. *Geophysical Research Letters* **46**:8952–8959.

Stauffer, G.,2004. NOAA protocols for groundfish bottom trawl surveys of the nation's fishery resources. US Department of Commerce, NOAA Technical Memorandum NMFS-F/SPO-65,205pp. http://spo.nmfs.noaa.gov/tm/

Stevenson, D. E., and G. R. Hoff. 2009. Species identification confidence in the eastern Bering Sea shelf survey (1982-2008). AFSC Processed Rep. 2009-04, 46 p. Alaska Fish. Sci. Cent., NOAA, Natl. Mar. Fish. Serv., 7600 Sand Point Way NE, Seattle WA 98115.

Stevenson, D. E., and R. R. Lauth. 2012. Latitudinal trends and temporal shifts in the catch composition of bottom trawls conducted on the eastern Bering Sea shelf. *Deep Sea Research Part II: Topical Studies in Oceanography* **65–70**:251–259.

Stevenson, D. E., and R. R. Lauth. 2019. Bottom trawl surveys in the northern Bering Sea indicate recent shifts in the distribution of marine species. *Polar Biology* **42**:407–421.

Taylor, B. M., and P. J. Diggle. 2014. INLA or MCMC? A tutorial and comparative evaluation for spatial prediction in log-Gaussian Cox processes. *Journal of Statistical Computation and Simulation* **84**:2266–2284.

Thorson, J. T. 2019. Measuring the impact of oceanographic indices on species distribution shifts: The spatially varying effect of cold-pool extent in the eastern Bering Sea.

Limnology and Oceanography **64**:2632–2645.

Wang, L., L. A. Kerr, N. R. Record, E. Bridger, B. Tupper, K. E. Mills, E. M. Armstrong, and A. J. Pershing. 2018. Modeling marine pelagic fish species spatiotemporal distributions utilizing a maximum entropy approach. *Fisheries Oceanography* **27**:571–586.

Ward, E. J., L. A. K. Barnett, S. C. Anderson, C. J. C. Commander, and T. E. Essington. 2022. Incorporating non-stationary spatial variability into dynamic species distribution models. *ICES Journal of Marine Science* **79**:2422–2429.

Winfree, R., J. W. Fox, N. M. Williams, J. R. Reilly, and D. P. Cariveau. 2015. Abundance of common species, not species richness, drives delivery of a real-world ecosystem service. *Ecology Letters* **18**:626–635.

Wyllie-Echeverria, T., and W. S. Wooster. 1998. Year-to-year variations in Bering Sea ice cover and some consequences for fish distributions. *Fisheries Oceanography* **7**:159–170.

Young, M. A., P. J. Iampietro, R. G. Kvitek, and C. D. Garza. 2010. Multivariate bathymetry-derived generalized linear model accurately predicts rockfish distribution on Cordell Bank, California, USA. *Marine Ecology Progress Series* **415**:247–261.

Zuur, A. F., I. D. Tuck, and N. Bailey. 2003. Dynamic factor analysis to estimate common trends in fisheries time series. *Canadian Journal of Fisheries and Aquatic Sciences.* **60**(5): 542-552.

7. APPENDIX

Appendix 1.1 Table of presence/absence models considered. All Spatiotemporal models were fitted with a Random Walk (RW) structure.

Response Variable	Covariate	Species	Model Type
Presence/absence	Depth	*Boltenia*	Spatial
Presence/absence	Depth	*Boltenia*	Spatiotemporal
Presence/absence	Temperature	*Boltenia*	Spatial
Presence/absence	Temperature	*Boltenia*	Spatiotemporal
Presence/absence	None	*Boltenia*	Spatial
Presence/absence	None	*Boltenia*	Spatiotemporal
Presence/absence	Depth	*Halocynthia*	Spatial
Presence/absence	Depth	*Halocynthia*	Spatiotemporal
Presence/absence	Temperature	*Halocynthia*	Spatial
Presence/absence	Temperature	*Halocynthia*	Spatiotemporal
Presence/absence	None	*Halocynthia*	Spatial
Presence/absence	None	*Halocynthia*	Spatiotemporal
Presence/absence	Depth	*Styela*	Spatial
Presence/absence	Depth	*Styela*	Spatiotemporal

Presence/absence	Temperature	*Styela*	Spatial
Presence/absence	Temperature	*Styela*	Spatiotemporal
Presence/absence	None	*Styela*	Spatial
Presence/absence	None	*Styela*	Spatiotemporal
Presence/absence	Depth	All	Spatial
Presence/absence	Depth	All	Spatiotemporal
Presence/absence	Temperature	All	Spatial
Presence/absence	Temperature	All	Spatiotemporal
Presence/absence	None	All	Spatial
Presence/absence	None	All	Spatiotemporal

Appendix 1.2 Table of CPUE models considered.

Response Variable	**Covariate**	**Species**	**Model Type**
CPUE	Depth	*Boltenia*	Spatial
CPUE	Depth	*Boltenia*	Spatiotemporal
CPUE	Temperature	*Boltenia*	Spatial
CPUE	Temperature	*Boltenia*	Spatiotemporal
CPUE	None	*Boltenia*	Spatial
CPUE	None	*Boltenia*	Spatiotemporal
CPUE	Depth	*Halocynthia*	Spatial
CPUE	Depth	*Halocynthia*	Spatiotemporal
CPUE	Temperature	*Halocynthia*	Spatial
CPUE	Temperature	*Halocynthia*	Spatiotemporal
CPUE	None	*Halocynthia*	Spatial
CPUE	None	*Halocynthia*	Spatiotemporal
CPUE	Depth	*Styela*	Spatial
CPUE	Depth	*Styela*	Spatiotemporal
CPUE	Temperature	*Styela*	Spatial
CPUE	Temperature	*Styela*	Spatiotemporal
CPUE	None	*Styela*	Spatial
CPUE	None	*Styela*	Spatiotemporal
CPUE	Depth	All	Spatial
CPUE	Depth	All	Spatiotemporal
CPUE	Temperature	All	Spatial
CPUE	Temperature	All	Spatiotemporal
CPUE	None	All	Spatial
CPUE	None	All	Spatiotemporal

Appendix 2: R code for spatiotemporal models

Run with R version 4.2.0

Rstudio 2022.02.3+492

2.1 To make the meshes for each species complex:

```
Meshspecies<- make_mesh(species.zeros, xy_cols=c("X","Y"), cutoff = 50)
```

2.2 Spatial, Spatiotemporal, and Spatiotemporal with Environmental Covariate

2.2.1 Spatial Information (No Covariates)

```
mspecies1 <- sdmTMB(
  data = species.zeros,
  formula = CPUE_weight_kgperhect ~ 1,
  mesh = meshspecies,
  family = tweedie(link = "log"),
  spatial = "on”
)

mspecies1
```

2.2.2 Spatiotemporal (No Covariates)

```
mspecies2 <- sdmTMB(
  data = species.zeros,
  formula = CPUE_weight_kgperhect ~ 1,
  mesh = meshspecies,
  family = tweedie(link = "log"),
  spatial = "on",
  time = "YEAR",
 spatiotemporal = "RW"
)

mspecies2
```

2.2.3 Spatiotemporal, Temperature as a Covariate

```
mspeciestemp<- sdmTMB(
  data = species.zeros,
  formula = CPUE_weight_kgperhect ~ GEAR_TEMPERATURE,
  mesh = meshspecies,
  family = tweedie(link = "log"),
  spatial = "on",
  time = "YEAR",
 spatiotemporal = "RW"
)
```

```
Mspeciestemp
```

2.3 Making Predictions on Model output

```
Predictionsmspecies1<- predict(mspecies1, newdata = speciesnewdata, type = "link")
```

Speciesnewdata being the grid created from sequences of original data (species.zeros) with appropriate variables brought over (lat, long, year, depth, etc). Type argument specifies the unit on the estimates, the default is type = “link” which estimates CPUE transformed to whichever link was selected (in this case log).

2.4 Mapping Predictions

```
mspecies1plot<-ggplot(predictionsmspecies1, aes(X, Y)) +
  geom_raster(aes(fill = est))
```

2.5 Cross Validation

```
mspecies1_cv <- sdmTMB_cv(
  CPUE_weight_kgperhect~1,
  data = species.zeros, mesh = meshspecies,
  family = tweedie(link = "log"),
  spatial = "on",
  time = "YEAR",
  k_folds = 8
)
```

To pull out estimated log predictive density and summed log likelihood

```
mspecies1_cv$elpd
mspcies1_cv$sum_loglik
```